Chapter 2
Introduction to Chemical Kinetics

Abstract After introducing the basis of the Arrhenius equation and its relationship to transition-state theory, forms of global chemical kinetic models are summarized, including shrinking core and pseudo *n*th-order reactions; sigmoidal reactions such as sequential, random scission, autocatalytic, logistic, and nucleation-growth model; and distributed reactivity models, including continuous and discrete activation energy distribution models. Isoconversional and model fitting methods for deriving chemical kinetic models are described, including how to use simple kinetic analyses to derive initial guesses for nonlinear regression of complex models. Common errors that lead to erroneous Arrhenius parameters are outlined.

Keywords Isoconversional · Model fitting · Prout-tompkins model · Sigmoidal reactions · Autocatalytic reactions · Random scission reactions · Distributed reactivity model · DAEM

Chemical kinetics describe of the rate at which chemical structures change. Chemical kinetics can be fundamental (involving quantum mechanics, statistical mechanics, or both) or phenomenological (semi-empirical rate laws derived from simplified physical models). The latter are often also called global kinetics or engineering kinetics, because they are derived primarily for application purposes instead of a truly fundamental understanding. They usually deal with lumped species and reactions, that is, reactions that represent the net progress of a set of related reactions. This chapter and book address phenomenological kinetics. An important warning up front is that there are probably more bad published papers on phenomenological (global) kinetics than good ones, so an understanding of this field is necessary to separate the wheat from the chaff. Results are presented for non-fossil fuels to demonstrate various reaction characteristics that should be considered for fossil fuels.

A.K. Burnham, *Global Chemical Kinetics of Fossil Fuels*,
DOI 10.1007/978-3-319-49634-4_2

2.1 The Activation Energy and Frequency Factor

Most reactions must traverse an energy barrier to change from one chemical structure to another, as shown schematically in Fig. 2.1. E_f and E_r are the forward and reverse activation energies. A reaction can be unimolecular (one chemical breaking down) or multi-molecular. It can either absorb heat (endothermic) by forming products with weaker bonds or emit heat (exothermic) by forming products with stronger bonds. The amount of heat absorbed or emitted is the enthalpy, which equals the difference between the forward and reverse activation energies, ΔE, at least within the simplified view of Fig. 2.1.

The reaction rate typically increases exponentially with increasing temperature in a fashion first parameterized by Arrhenius in 1889 [1]. Specifically, the rate constant k increases according to the formula

$$k = Ae^{-E/RT}, \tag{2.1}$$

where A is a frequency factor, as it has units of reciprocal time in addition to other units, depending on the kind of reaction, E is the activation energy for the reaction, R is the universal gas constant, and T is the absolute temperature. R has a value of 1.987 cal/(mol K) or 8.314 J/(mol K), depending on the units chosen for energy. In

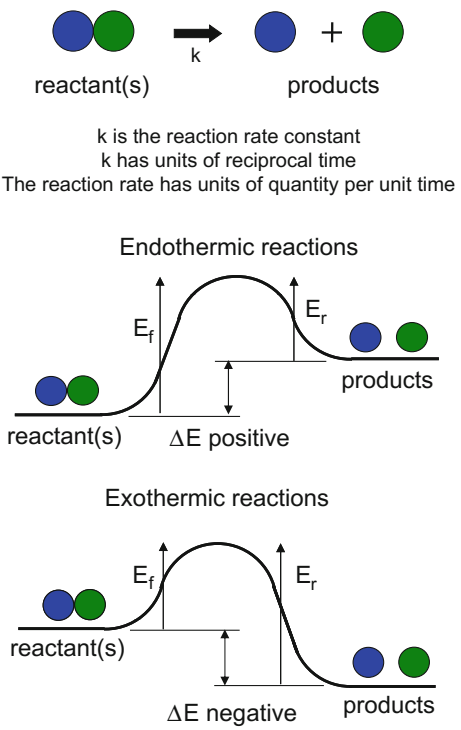

Fig. 2.1 Schematic representation of the chemical reaction barrier

practice, it is far simpler to use activation energies in Kelvins to avoid a set of unit conversions and multiplications during usage.

The reason for this temperature dependence is shown simplistically in Fig. 2.1. At any given temperature, molecules have a statistical distribution of energies, commonly a Boltzmann distribution [2]. For most reactions, only a small fraction of the molecules have enough energy to get over the energy barrier of the reaction. That fraction increases with temperature. For a bimolecular reaction, the fraction depends on the fraction of molecules having a velocity greater than some threshold value in the Maxwell-Boltzmann distribution [3]. For unimolecular decomposition, the Boltzmann distribution describes the probability that a given bond will be in an energetic-enough state to dissociate. Some reactions have no reaction barrier—notably free-radical recombination reactions, which are important in hydrocarbon cracking.

Multi-molecular gas-phase reactions typically have power-law temperature dependence in addition to the exponential dependence to account for collision frequency

$$k = AT^b e^{-E/RT}, \tag{2.2}$$

where b is ranges from 0.5 to 1.5. However, one has to traverse several hundred degrees before pre-exponential temperature dependence has any practical significance. Burnham and Braun [4] give the example of an ideal linear temperature coefficient absorbed into an effective activation energy. Over a 50 °C range, the effective activation energy predicts the true temperature dependence to an accuracy of one part in 10^4. Extending that example, the reaction rate predicted by the effective rate constant is within 10 % of the ideal value over a 700 °C range. Given that the error is only in one direction, the overall error could be reduced to no more than 5 % by not requiring exact agreement at the calibration temperature. Using a pre-exponential temperature dependence makes sense only when it is known from first principles, and that is commonly the case for detailed mechanistic modeling of hydrocarbon pyrolysis and combustion reactions.

The reaction rate constant is often characterized by transition-state theory [5], which hypothesizes an activated complex at the peak of the reaction barrier. The enthalpy of formation of that activated complex, ΔH, is the activation energy. For unimolecular decomposition reactions, the frequency factor is related to the vibrational frequency of the bond to be broken in the active complex and is a function of Boltzmann's constant, k_b, Planck's constant, h, the absolute temperature, and the entropy of formation of the activated complex, ΔS. This gives a rate constant

$$k = \left(\frac{k_B T}{h}\right) e^{-\Delta G/RT} = \left(\frac{k_B T}{h}\right) e^{\Delta S/R} e^{-\Delta H/RT}. \tag{2.3}$$

For typical pyrolysis temperatures, the $k_B T/h$ is a little over 10^{13} s^{-1}, and the entropy term is often ignored.

While some people studying complex reactions in a phenomenological or global manner refer to transition-state theory and activated complexes, such references are usually ill-placed and more often give an indication that the person is naïve concerning the huge simplifications involved in their work relative to fundamental reaction mechanisms.

For a simple unimolecular decomposition reaction, the activation energy is equal to the energy of the bond to be broken. However, such simple reactions are rarely of practical interest. Instead, reactions of interest, especially for fossil fuels, involve chains of reactions. For example, if a normal hydrocarbon splits into two fragments, the activation energy of that initiation reaction is equal to the strength of a carbon-carbon bond, or about 82 kcal/mol. However, the molecular fragments are unstable and can either split an ethylene molecule off their end or start attacking their neighbors by abstracting a hydrogen atom from the middle of a neighboring chain, thereby converting a primary free radical to a more stable secondary free radical. In the latter case, the secondary free radical can decompose into an alkene and another primary free radical. These latter steps are called propagation reactions. Sometimes two free radicals run into each other and form a stable hydrocarbon, often branched. This is called a termination reaction and usually has zero activation energy. Since the breaking of one strong bond results through a chain reaction to break many bonds through propagation reactions, which have lower activation energies, the overall activation energy for hydrocarbon cracking is in the range of 50–60 kcal/mol, dependent upon reaction conditions.

2.2 Introduction to Conversion and Pressure Dependence

It is commonly assumed for practical purposes that the dependences on conversion, temperature, and pressure can be separated [6]. Before proceeding, it should be understood that chemical reaction networks are expressed as differential equations describing the disappearance and appearance of reactants and products. Many reactions of interest are expressed as a single differential equation giving the rate law for reactants going to products, and in this case, some write the rate law in terms of disappearance of reactants, x or some other symbol, and some use the appearance of products, α. Obviously, $x = 1 - \alpha$.

The resulting differential equations for either x or α are given in equations

$$dx/dt = -k(T)f(1-x)h(P) \tag{2.4}$$

and

$$d\alpha/dt = k(T)f(\alpha)h(P). \tag{2.5}$$

where P is pressure. Functions for $f(\alpha)$ and the integral form, $g(\alpha)$, are commonly tabulated in the thermal analysis literature for solid-state reactions, where

$$g(\alpha) = \int_0^{\alpha} \frac{d\alpha}{f(\alpha)}. \tag{2.6}$$

One selection of such functions is given in Table 2.1. These equations deal with situations involving nucleation-growth characteristics, shrinking cores, intraparticle diffusion resistance, and distributed reactivity (e.g., power law in time). The Avrami-Erofe'ev and Prout-Tompkins models are alternative mathematical approaches to treat sigmoidal reactions (nucleation-growth), and they can also be used for generalized initiation-propagation reactions. The Jander and Ginstling-Brounshtein (G-B) equations are included for completeness and are reasonably accurate up to about 50 % conversion, but more accurate equations for planar, cylindrical and spherical particles have been derived [7].

The *h(P)* function can be empirical or fundamentally based, and separating the pressure dependence is an approximation that is not always valid. The most obvious example of pressure dependence is for a gas-solid reaction, for which the reaction rate depends on the gaseous reactant partial pressure. The pressure dependence could be, for example, a power law or some type of adsorption isotherm [8]. Another common example where it does work is a reversible mineral decomposition, e.g., $CaCO_3 \leftrightarrow CaO + CO_2$, where $h(P) = 1 - P/P_{eq}$, P is the gaseous product partial pressure, and P_{eq} is the equilibrium vapor pressure. However, there are other cases where the pressure dependence is not truly separable. In hydrocarbon cracking, a change in pressure changes relative amounts of initiation, propagation, and termination reactions, which leads to a change in the global activation energy [9]. Another example is where increasing pressure modestly accelerates the reaction rate due to increased autocatalysis [10], whereas increasing pressure greatly decelerates the

Table 2.1 Selection of commonly used kinetic models

Reaction model	Code	Differential form, $f(\alpha)$	Integral form, $g(\alpha)$
1st order	F1	$1 - \alpha$	$-\ln(1 - \alpha)$
Pseudo *n*th order	Fn	$(1 - \alpha)^n$	$1/(n-1)[(1 - \alpha)^{(1-n)} - 1]$
Contracting cylinder	R2	$2(1 - \alpha)^{1/2}$	$1 - (1 - \alpha)^{1/2}$
Contracting sphere	R3	$3(1 - \alpha)^{2/3}$	$1 - (1 - \alpha)^{1/3}$
Power law	Pv	$v\alpha^{(v-1)/v}$	$\alpha^{1/v}$
Avrami-Erofe'ev	Ap	$p(1 - \alpha)[-\ln(1 - \alpha)]^{(p-1)/p}$	$[-\ln(1 - \alpha)]^{1/p}$
Extended Prout-Tompkins	ePT or Bna	$(1 - \alpha)^n\alpha^m$	No analytical solution
1D diffusion	D1	$\frac{1}{2}\,\alpha^{-1}$	α^2
2D diffusion	D2	$[-\ln(1 - \alpha)]^{-1}$	$(1 - \alpha)\ln(1 - \alpha) + \alpha$
3D diffusion (Jander)	D3	$3/2(1 - \alpha)^{2/3}[1 - (1 - \alpha)^{1/3}]^{-1}$	$[1 - (1 - \alpha)^{1/3}]^2$
3D diffusion (G-B)	D4	$3/2[(1 - \alpha)^{-1/3} - 1]$	$1 - 2\alpha/3 - (1 - \alpha)^{2/3}$

There is some variation in the code nomenclature and location of the constants in the integral and differential forms

reaction rate due to increased diffusion resistance [11]. Pressure can also appear in an activation volume term, which can be interpreted as an entropic contribution to the transition-state free energy, but it is very hard to uniquely identify such contribution for a complicated reaction system [12]. Pressure dependence will be taken up again in later chapters.

Equations (2.4) and (2.5) also assume that one starts with a material that is homogeneous. Materials of interest often have moieties with different reactivity. Consequently, it is often appropriate to divide the reaction into a set of independent parallel reactions, with or without the same pressure dependence:

$$dx_i/dt = -k_i(T)f(1 - x_i). \tag{2.7}$$

The sum of the initial x_i equals one. The parallel reaction model can be extended from a set of discrete reactions to a continuous distribution. Three common continuous distributions are Gaussian [13], Weibull [14] and Gamma distributions [15]. The Gaussian distribution has the disadvantage of being symmetric, but a Gaussian distribution of *n*th-order reactions can achieve similar fits to the Weibull distribution [4].

Reactions are often grouped into three classes: acceleratory, decelerator, and sigmoidal. Sigmoidal reactions have an acceleratory phase followed by a decelerator phase. In fact, chemical reactions with purely acceleratory character are rare. A solid-state reaction that starts in the center of a sphere and then propagates outward is an ideal example. A chain-branching reaction with a branching ratio greater than one is another example. Runaway nuclear fission is a non-chemical example of such an acceleratory reaction. Decomposition of nitro energetic materials initially accelerates due to autocatalysis, but if the released heat and pressure are allowed to dissipate, they turn decelerator and are then sigmoidal.

Most, if not all, reactions of interest in fossil fuels are either sigmoidal or decelerator. In contrast to the usual classification, it is useful to divide the decelerator reactions into three types: first-order reactions, whose reaction rates decay exponentially, those that decay faster than an exponential, and those that decay slower than an exponential. A plot of the logarithm of the reaction rate versus time distinguishes the three types, as shown in Fig. 2.2, which is adapted from Burnham and Braun [4].

In such a semi-log plot, *n*th-order reactions with $n < 1$ are concave downward, which means that the reactant disappears faster than predicted from an initial first-order reaction rate at low conversion. Pseudo *n*th-order reactions, with $n > 1$ are concave upward, which gives the opposite prediction. The adjective *pseudo* is introduced, because the reactions are not *n*th-order in the sense of traditional gas-phase or solution reaction kinetics. In these cases, reaction order is expressed in terms of partial pressure or concentration. For pseudo *n*th-order reactions, the reaction is parameterized in terms of reaction progress of a distinct phase, which is normalized to zero or one, depending on whether one is using fraction reacted or fraction remaining.

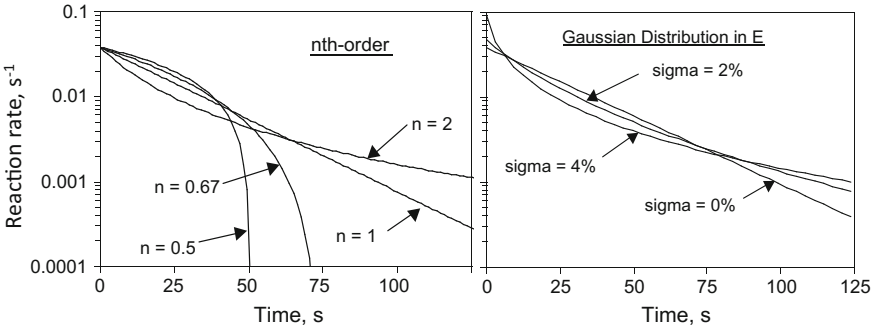

Fig. 2.2 Plot of the logarithm of the reaction rate versus time showing that some models decelerate faster than a first-order model and some decelerate slower. Adapted from Burnham and Braun [4] courtesy of LLNL

A Gaussian distribution in activation energy, which is not the same as a Gaussian distribution in k, is also concave upward, so it is similar in some respects to a pseudo nth-order reaction with $n > 1$. This is because a pseudo nth-order reaction is mathematically equivalent to having a Gamma distribution of frequency factors [4]. Consequently, pseudo nth-order reactions are a legitimate way of treating a reactivity distribution. Given that this book does not deal with traditional nth-order reactions, the *pseudo* adjective will usually be dropped for the duration of the book.

2.3 Integrating the Reaction Rate

While some reaction models can be integrated exactly for isothermal conditions, most experiments and applications of practical interest involve either reaction models or thermal histories for which an exact analytical solution is not available. This section discusses the mathematical methods needed to deal with this situation. This section closely follows Burnham and Braun [4].

The first concept is that there are generally two types of modeling of interest. The first is exploratory modeling, and the second is application modeling. Exploratory modeling explores various concepts using fast and flexible tools where the ultimate in accuracy is not required. Application modeling uses more mature models that have been programmed with more sophisticated and accurate numerical methods. Often, the application modeling is done by someone other than the computer code developer, so changes are more difficult. Numerical methods for both types of activities are presented in this section.

A second concept is that neither isothermal nor constant-heating-rate conditions occur in real-life applications. In fact, it is even hard to do truly isothermal experiments over the range of temperatures of interest, particularly considering that

it is important to achieve high conversions over the entire range of temperatures to fully characterize the reaction mechanism. Consequently, most of the literature developing equations and algorithms for strictly isothermal or strictly constant heating rates must be viewed as too limiting for modern computers. Once the simple scoping calculations are done, it is just as easy to program highly accurate algorithms that work for any arbitrary thermal history.

The starting point for all algorithms involving either a single reaction or a set of parallel independent reactions is the integration Eq. (2.4) or (2.5) over time. This approach does not use the assumption that k is constant, as does Eq. (2.6). The following expression uses fraction remaining (2.4) rather than fraction reacted (2.5):

$$x = \int_0^t k(T(t))f(1-x)dt. \tag{2.8}$$

For first and nth-order reactions, respectively, this equation evolves to

$$x = \exp\left[-\int_0^t k(T(t))dt\right] \tag{2.9}$$

and

$$x = \left[1-(1-n)\int_0^t k(T(t))dt\right]^{1/(1-n)}. \tag{2.10}$$

For isothermal conditions, k is constant, so one obtains the familiar equations

$$x = \exp[-kt] \tag{2.11}$$

and

$$x = [1-(1-n)kt]^{1/(1-n)}. \tag{2.12}$$

In the middle of the 20th century, it became fashionable to conduct kinetic experiments using a constant heating rate to avoid the transient heat-up time characteristic of isothermal experiments. At a constant heating rate, $dT/dt = \beta$, and defining $y = E/RT$, Eq. (2.10) becomes

$$x = \exp\left[-\frac{AE}{\beta R}\int_y^\infty \frac{\exp(-y)}{y^2}dy\right]. \tag{2.13}$$

The inside integral over y, often called the "Temperature Integral," does not have an exact analytical solution. With a change of variables, it can be converted to the well-known exponential integral that has many approximate solutions to any desired accuracy. Numerous papers in the thermal analysis literature have explored various approximations, and Flynn [16] gives a fairly complete review of that work.

He also addresses alternate forms of the rate law. The most interesting alternative to the conventional approach is that adding T^2 to the pre-exponential factor leads to an exact solution for a constant heating rate, which obviously has some justification as discussed in the context of the previous section, but the case is not strong enough to include it, given that dealing with the integral is not very difficult. Its solution can be expressed as an infinite series as follows:

$$x = \exp\left[-\frac{ART^2}{\beta E}\left(1 - \frac{2RT}{E} + \cdots\right)e^{-\frac{E}{RT}}\right]. \tag{2.14}$$

Although some German coal workers [17] and early LLNL oil shale papers [18] take only the unity term, a more common approximation, generally attributed to Coats and Redfern [19], is to include the $2RT/E$ term as well. This gets one most of the way to the exact solution for large values of E/RT. Even so, Flynn criticizes this approximation and says that it leads to publication of incorrect activation energies. However, while better, yet still simple, approximations are available [20], e.g., $(1 + 2RT/E)^{-1}$ and $(1 + 4RT/E)^{-0.5}$, there are usually far more serious problems causing inaccurate activation energies. Nevertheless, programming one of the simple alternatives for scoping calculations is just as easy, so it might as well be done.

The more important issue is the single-minded advocacy of higher level, more complicated approximations to the Temperature Integral. Rational approximations up to the eighth degree achieve essentially perfect accuracy [21, 22]. However, concentrating on only the constant-heating-rate numerical solution misses the real issue for deriving chemical kinetics—it is best to use a variety of heating schedules, including nominally isothermal, constant heating rate, and even oscillatory ramps [16] to get the most stringent test of any kinetic model. For this purpose, it is far superior to adopt the approach of Braun and Burnham [23] that divides any complex thermal history into a series of constant-heating-rate segments. Consider the integration of the rate constant in Eqs. (2.9) and (2.10) as being broken into a series of such steps:

$$\int_0^t k(T(t))dt = \sum\nolimits_{i=0}^{n} \int_{t_{i-1}}^{t_i} k(T(t))dt, \tag{2.15}$$

where

$$\int_{t_{i-1}}^{t_i} k(T(t))dt = \frac{1}{\beta}\left\{T_i k_i\left[1 - \frac{\left(y_i^2 + a_1 y_i + a_2\right)}{\left(y_i^2 + b_1 y_i + b_2\right)}\right] - T_{i-1}k_{i-1}\left[1 - \frac{\left(y_{i-1}^2 + a_1 y_{i-1} + a_2\right)}{\left(y_{i-1}^2 + b_1 y_{i-1} + b_2\right)}\right]\right\} \tag{2.16}$$

and $y = E/RT$, $a_1 = 2.334733$, $a_2 = 0.250621$, $b_1 = 3.330657$, and $b_2 = 1.681534$. Increased accuracy can be obtained using a five-term rational approximation [24], but such accuracy is a matter of diminishing returns in the case of applied kinetics

where the true mechanism is not known well. If the heating rate, β, is zero (isothermal), one can use either the isothermal solution or an extremely low heating rate so that the change in temperature over the longest isothermal segment is a small fraction of a degree.

For a first-order reaction, there is a very simple method to get a good estimate for the extent of reaction over any thermal history. It takes advantage of the fact that the amount of reactant over each increment of time is simply the exponential of the time interval times the average rate constant over the integral, specifically

$$\frac{x_i}{x_{i-1}} = \exp\left[-(t_i - t_{i-1})\left(A_i e^{-E_i/RT_i} + A_{i-1} e^{-E_{i-1}/RT_{i-1}}\right)/2\right]. \tag{2.17}$$

Here a provision is made for a variable frequency factor as could be derived from isoconversional kinetic analysis methods, in which A and E pairs are determined as a function of conversion as described in the next section. That makes the calculation of the average rate constant over the interval a little more complicated—an iterative process for best accuracy—but the principle is simple. Regardless of whether A and E are independent of conversion or not, the total extent of reaction is simply

$$x_i = \Pi_i \exp\left[-\Delta t_i k_{avg,i}\right] = \exp\left[-\sum\nolimits_i \Delta t_i k_{avg,i}\right] \tag{2.18}$$

There are many other ways to integrate differential equations, ranging from a 1-step explicit integration that does surprising well for small step sizes to multistep implicit methods. A review of and instruction in numerical integration is outside the scope of this book, and there are numerous texts on the subject. An advantage of numerical integration over any of the methods discussed here is that any rate law can be integrated without consideration of whether an analytical solution exists, and systems of kinetic equations can be integrated as well. Various numerical integration packages are available, and LSODE [25] is the package used in many applications developed at LLNL and elsewhere.

2.4 Methods of Kinetic Analysis

There are basically two types of methods for deriving a kinetic expression for a condensed phase reaction—isoconversional analysis and model fitting. Both have advocates, but since both have advantages and disadvantages, they are best used in concert. Inconsistent activation energies from the two methods should raise a red flag.

2.4.1 Isoconversional Methods

Isoconversional methods start with Eq. (2.4) or (2.5) with $h(P)$ assumed to be unity. Isoconversional methods are sometimes called model-free kinetics, because they do not involving fitting to a phenomenological model, but they are not assumption free. The basic assumption is that at any given extent of reaction, the same reactions occur in the same ratio independent of temperature. It is easy to construct reaction networks that do not follow the isoconversional principle. One example is a set of parallel independent reactions that change in relative reactivity as a function of temperature due to different activation energies [26]. Another example is the case of competitive reactions with different activation energies, which causes the overall reaction pathway to be different at different temperatures [27]. Nevertheless, some isoconversional methods usually work pretty well and should be part of the toolkit for developing a robust kinetic model. See Vyazovkin [28] for a thorough discussion of various approaches and applications.

Isoconversional methods were developed about 50 years ago. Friedman first developed the differential method [29]. Ozawa and Flynn and Wall independently developed the integral method [30, 31]. Flynn gives a couple short but educational discussions of development of the integral methods [32, 33]. The general concept is shown graphically in Fig. 2.3.

Friedman assumed no pressure dependence and differentiated Eq. (2.4) to obtain

$$\ln\left(-\frac{dx}{dt}\right) = \ln A + \ln f(x) - E/RT \tag{2.19}$$

He then stated that $f(x)$ can be assumed to be constant for constant values of x, the definition of isoconversional, which he states is true if the chemical pathway is

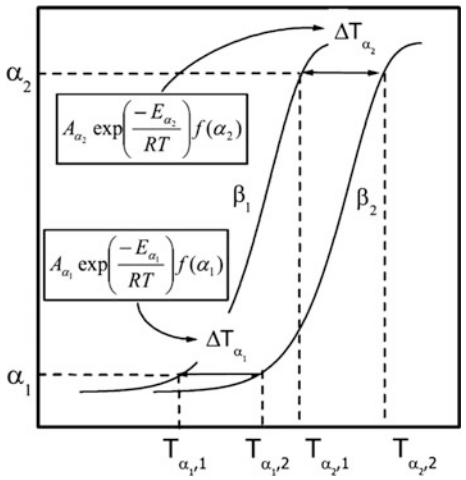

Fig. 2.3 Graphical representation of the isoconversional kinetic analysis concept from Vyazovkin et al. [6]. Reprinted with permission. © Elsevier

independent of temperature. Plotting the natural log of the reaction rate versus $1/T$ gives a slope of E/R and an intercept of $\ln[Af(x)]$. He further noted that if the reaction is nth order, a plot of $\ln[Af(x)]$ versus $\ln(x)$ would be linear with a slope of n and an intercept of $\ln(A)$. In practice, E/R is frequently not constant over x, and the plot to determine n is rarely linear, so the value of the method is different than originally envisioned, as will be explained below.

Friedman originally derived his isoconversional method using fraction remaining, x, but the normal convention in thermal analysis is to use fraction reacted, α. Consequently, the intercept is normally given as $\ln[Af(\alpha)]$. Regardless, the function is the same, and one can find $f(x)$ from Table 2.1 by merely substituting x for $1 - \alpha$. For a first-order reaction, $f(x) = x = 1 - \alpha$, so A is merely the intercept divided by the fraction remaining. If the conversion steps are small enough, those effective first-order frequency factors can be used for each instantaneous reaction rate and incremental fraction reacted.

Ozawa and Flynn and Wall independently observed that the approximation of the temperature integral proposed by Doyle [34] leads to the equation

$$\ln(\beta_i) = \text{const} - 1.052E_\alpha/RT_{\alpha,i}. \tag{2.20}$$

This is known as the OFW equation. Plotting $\ln(\beta_i)$ versus $1/T_i$ at conversion α gives a slope of E/R at that α.

A more accurate simplification of the temperature integral leads to the KAS (Kissinger-Akahira-Sunose) equation [35]:

$$\ln\left(\beta_i/T_{\alpha,i}^2\right) = \ln[\frac{\mathrm{A}_\alpha R}{E_\alpha g(\alpha)}] - E_\alpha/RT_{\alpha,i}. \tag{2.21}$$

Slightly more accurate activation energies can be obtained by replacing the square of the temperature with a power of 1.92 and adding a coefficient of 1.0008 in front of the right-hand term [36], but this still does not address the issue that the equation assumes that E_α is constant, and it rarely is. Vyazovkin [37] addresses this issue by integrating the time or temperature integral in a way that the activation energy is assumed to be constant only over small steps.

$$\mathrm{J}[E_\alpha, T(t_\alpha)] = \int_{t_{\alpha-\Delta\alpha}}^{t_\alpha} \exp\left[\frac{-E_\alpha}{RT(t)}\right] dt. \tag{2.22}$$

Vyazovkin's advanced integral method obtains activation energies practically identical to those obtained by Friedman's method [6].

For completeness and historical perspective, it is important to recognize the Coats-Redfern equation and its adaptation to an isoconversional method. The original Coats-Redfern method [19] fitted data from a single heating rate to the equation

$$\ln\left[\frac{\ln(x)}{T^2}\right] = -\frac{E}{RT} + ln\left[-AR\left(1-\frac{2RT}{E}\right)\beta E\right]. \tag{2.23}$$

This method is highly inaccurate and has been strongly discouraged by recent ICTAC papers on kinetic analysis [6, 38]. Even so, this equation can be converted into an isoconversional method by rearrangement [6]:

$$\ln\left[\beta_i/\left(T_{\alpha,i}^2\left(1-\frac{2RT}{E}\right)\right)\right] = \ln[-A_\alpha R/(E_\alpha \ln(x))] - E_\alpha/RT_{\alpha,i}. \tag{2.24}$$

This must be solved by iteration until convergence by substituting previous values of E_α into the $1 - E/RT$ term. Further improvement in the method could be obtained by using more accurate approximations for the $1 - E/RT$ term, but again, this is a matter of diminishing returns, as the equation is fundamentally limited by the assumption of constant activation energy when the purpose is often to determine the conversion dependence of the activation energy.

One final isoconversional method to be mentioned only briefly at this point is the model of Miura et al. [39, 40] He follows much earlier work by Vand [41] arguing that due to overlapping parallel reactions that make up the reactivity distribution, an effective fraction reacted rather than the actual fraction reacted should be used in isoconversional methods. This method is discussed further in a later section.

Once the fundamental limitations were recognized for all integral isoconversional methods except the advanced integral method, a recurring debate in the thermal analysis community is whether the rate method or advanced integral method is superior in view of the fact that real data have noise, both in terms of random instrument noise and uncertainty in baselines.

In principle, integral data can be differentiated and rate data can be integrated, but errors can be introduced by both differentiation and integration if not done properly. A minimum requirement of any method is that successive differentiation and integration of integral data must recover the original integral data (except, of course, the initial value, as it corresponds to a constant baseline), and the corresponding recovery of rate data from cyclic integration and differentiation.

Next, one can smooth rate data to reduce noise, but only to the extent that one wants to resolve variations in A and E as a function of conversion. Resolution down to 10 % conversion increments is adequate for some qualitative purposes, but resolution down to 1 % increments is desirable for application modeling purposes. Obviously, the original data must have at least 100 points over the conversion interval for the latter analysis, and that is commonly available from thermal analysis instruments.

One suggestion is that it is best to use integral methods on integral data (e.g., weight loss and product accumulation) and differential methods for rate data (e.g., differential scanning calorimetry and gas evolution). However, I have experience only using Friedman's methods to derive kinetics for application purposes from both integral and rate data (using both the LLNL Kinetics2015 [42] and AKTS

Thermokinetics [43] programs) and do not see any fundamental limitations in using Friedman's method for both as long as the data are of high quality.

One final note is that when using isoconversional kinetics for applications, isoconversional kinetics should really be classified as an infinitely sequential model. One can assume, for example, that each small increment of conversion is governed by a first-order reaction and derive the first-order frequency factor. Then the extent of conversion over any thermal history is merely a series of first-order reactions over the conversion intervals. This is a direct outgrowth of the isoconversional assumption—that the same reaction progress occurs, independent of temperature, and over each successive reaction interval.

Kissinger's method [44] is a very simple method that is not universally an isoconversional method but sometimes is and otherwise is usually close to it. It involves using the maximum of the reaction rate as a function of heating rate to derive an activation energy and pre-exponential factor. It is rigorously correct and isoconversional for first-order reactions. It is an excellent approximation for *n*th-order [45], nucleation-growth [46], and distributed reactivity reactions [23], although Vyazovkin et al. [6] discuss some cases where it does not work. It is important not to confuse Kissinger's $T_{\max}$ method with the KAS method, which is rigorously isoconversional. Kissinger's method is also known in the vacuum community as Redhead's method [47].

At the peak reaction rate, the derivative of the reaction rate (second derivative of conversion) is equal to zero. Differentiating Eq. (2.4) with $h(P) = 1$, setting it equal to zero, and eliminating a term outside the brackets yields

$$0 = \left[\frac{\beta E}{RT_{max}^2} + A\exp\left(\frac{-E}{RT_{max}}\right)\frac{df(x)}{dx}\right]. \tag{2.25}$$

For a first order reaction, $df(x)/dx = -1$, so

$$\ln\left(\frac{-\beta}{T_{max}^2}\right) = -\frac{E}{RT_{max}} + \ln\left(\frac{AR}{E}\right). \tag{2.26}$$

A few final comments are appropriate concerning the strengths and limitations of the isoconversional methods for fossil fuels. By their nature, isoconversional methods recognize the possibility of reaction heterogeneity, which implies that different products may be formed at different stages of the global conversion. If one merely wants to calculate to global conversion of a starting material, they are frequently as good as or better than model fitting, because they can more easily accommodate conversion dependence of both A and E. Burnham and Braun [4] discuss their use for coal pyrolysis, and Dieckmann [48] discusses their use for modeling petroleum formation. Section 4.4.2 shows how they help diagnose that dependence for typical oil-prone kerogens, and Sect. 7.1 shows how they predict a broader range of temperature for petroleum generation.

However, they do have limitations. If one wants to model differences in generated products as a function of conversion, it is not straightforward with

isoconversional methods. If one wants to model two different measures of reaction progress, the isoconversional kinetics for those measure can be completely different, e.g., weight loss and heat evolution for a material with overlapping endothermic and exothermic stages. Finally, isoconversional methods may not be appropriate for reaction intermediates, because the combination of generation and consumption reactions makes a simple definition of conversion difficult or impossible, depending on the complexity of the reaction network.

2.4.2 Model Fitting Methods

Model fitting can take several forms, but in the end, all methods involve minimizing the difference between a calculated and a measured conversion or rate as a function of some time and temperature.

Linear regression [49] involves minimizing the residual sum of squared differences for the simple equation, $y = mx + b$. The solution for m is simply

$$m = \frac{\left[\sum_i x_i y_i - \left(\sum_i x_i \sum_i y_i\right)/n\right]}{\left[\sum_i x_i^2 - \frac{\left(\sum_i x_i\right)^2}{n}\right]}. \tag{2.27}$$

The example of Kissinger's equation in Eq. (2.26) means plotting $\ln(\beta/T_{\max}^2)$ versus $1/T_{\max}^2$ gives the slope, m, of E/R. The same linear regression, of course, is the basis of all isoconversional methods.

The first measure of the quality of fit of a linear model is the correlation coefficient, r:

$$r^2 = \frac{\left[\sum_i x_i y_i - \left(\sum_i x_i \sum_i y_i\right)/n\right]}{\left\{\left[\sum_i x_i^2 - \frac{\left(\sum_i x_i\right)^2}{n}\right]\left[\sum_i y_i^2 - \frac{\left(\sum_i y_i\right)^2}{n}\right]\right\}}. \tag{2.28}$$

For a perfectly linear data set, $r^2 = 1$. Two realizations are shown in Fig. 2.4 for a Kissinger plot using Arrhenius parameters of 1.0×10^{14} s^{-1} and $E = 54{,}000$ cal/mol and maximum random error of ± 3 °C for each point for a heating range of 1–16 °C/min.

The frequency factor, A, changes in concert with E according to a compensation relationship. A more complete study of random errors on A and E is given elsewhere [50], and a rather detailed discussion of the respective contributions of random errors and mechanistic effects to the compensation effect has been presented recently [51, 52]. Rather than engaging is a detailed discussion of the compensation effect at this point, I merely mention that values of r^2 less than 0.98 indicate that the results should be used with caution outside the range of calibration. For reliable extrapolation from lab experiments to geological time and temperature

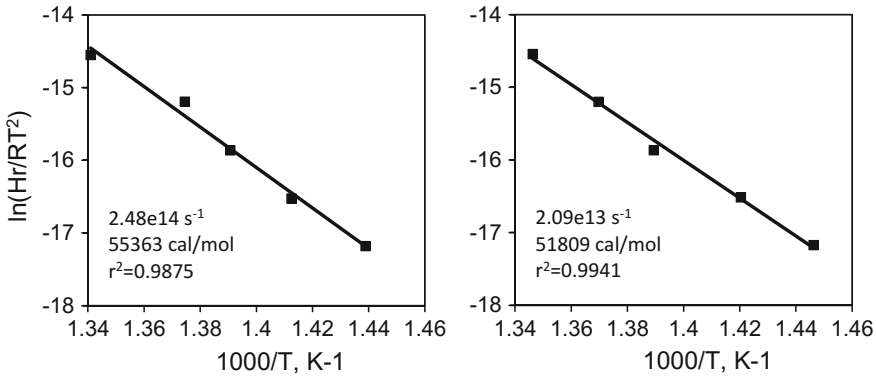

Fig. 2.4 Two realizations of a Kissinger plot including measurement noise

conditions, the r^2 must be greater than 0.997. The geological extrapolation issue is discussed in greater detail in Sect. 7.1. In addition, it is best to plot the residuals (differences between measured and calculated) versus the abscissa variable to inspect for non-random trends that would indicate the need for a higher order model.

Any model that can be transformed into a linear equation can be analyzed by linear regression. The most common example is a first-order reaction, for which the logarithms of the reaction rate and fraction remaining are linear with time. Such a transformation, however, introduces a problem that depends on the nature of the detection.

In most measurements of rates and fractions reacted (or remaining), there are both random errors in the measurement and an uncertainty in the baseline. Random errors can have components proportional to the maximum instrument sensitivity and the measured signal. Model fitting by linear transformation and regression magnifies error associated with baseline errors and noise that is proportional to maximum instrument sensitivity. Consequently, it effectively raises the relative importance (weighting) of the least reliable data. Taking the example of a first-order reaction with random errors of 2 % of maximum plus 2 % of the value plus a 2 % error in the baseline, the error in the rate constant from linear regression is 2.5 %, while the error in the nonlinear fit is 1.4 %. More details on linearization methods for optimizing kinetic models are given elsewhere [6].

Nonlinear regression [53] also involves minimizing some function of the difference between calculated and measured values, ordinarily the residual sum of squares (RSS):

$$\mathrm{RSS} = \sum\nolimits_i \left(y_{exp,i} - y_{calc,i}\right)^2. \tag{2.29}$$

Unlike the linear regression case, there is no analytical solution. Instead, the minimum value must be found by some type of search algorithm. One way is to

merely map out a surface with variations in the variables and look for the minimum by a grid search. Another method is to look at the derivative of the RSS with respect to changes in the different variables and move continuously toward the lowest value. One popular method of doing the latter is the Levenberg-Marquardt Algorithm [54], which is also known as damped least squares, alternating between gradient decent and Gauss-Newton methods.

Kinetics2015 and predecessors dating back to 1987 use the Levenberg-Marquardt algorithm for optimization. In one case, the discrete energy distribution model, optimization uses iterative linear regression and constrained non-linear regression optimization based on the Levenberg-Marquardt algorithm. Lakshmaman et al. [55] use a grid-search method, and Hillier et al. [56] use a simulated annealing method that has aspects similar to the grid-search method.

All nonlinear regression methods have the danger of falling into a local minimum rather than the global minimum. One method to check for such a problem is to start the minimization from a different set of initial conditions. Another method is to restart the minimization a few times to be sure that it cannot find a lower minimum. The latter is used by Kinetics2015, and the improvement is usually minor. More important is to start the non-linear regression with good initial guesses. The philosophy adopted by Kinetics2015 is to provide those initial guesses from simpler analyses such as isoconversional analysis. How that is done is explained in the following sections.

Another issue is the ability to fit multiple reactions to reaction data. This is relatively straightforward, for example, if for a constant heating rate, two fairly well resolved peaks are observed. Even so, sometimes it is useful to do successive optimizations with subsets of the parameters prior to a final optimization with parameters that are close to the final values. More serious is when some system of parallel, sequential, and competing reactions does not give distinctive features to insure a unique fit. The Netzsch Thermokinetics [57] software has the capability to construct such complex models. If some reaction parameters can be fixed reliably by other considerations, the probability of achieving a defendable model improves.

A final consideration is that many people want a universally applicable measure of goodness of fit like r^2. It does not exist for non-linear regression. While linearization methods are sometimes used to estimate parameter uncertainties in nonlinear regression, they may be grossly in error unless the model is close to linear [58]. When running a set of similar optimizations, one can compare the normalized residual sum of squares for a comparison within that set. Another indicator would be to change one parameter with the others fixed to cause the residual sum of squares to change by some amount deemed to be within the experimental reproducibility of the minimum, then re-optimize the other variables with that variable fixed [59]. Roduit et al. [60] present a statistical test for whether adding another parameter is justifiable in terms of the improvement in the residual sum of squares.

2.5 Sigmoidal Reaction Models

As mentioned in the previous section, the isothermal reaction rate of sigmoidal reactions is initially small, gradually accelerates with time as some intermediate property controlling the reaction rate increases, then gradually decreases to zero as the reactants are consumed. In integrated form it looks like a horizontally stretched "S", with a maximum slope at some intermediate conversion. Because there is always a finite heat-up time for a pyrolysis reaction, the reaction rate and conversion have some sigmoidal characteristics from the acceleration of the reaction with temperature, and a careless analyst may dismiss this acceleratory phase as sample heat-up, but it is truly a fundamental characteristic of many chemical reactions.

Sigmoidal reactions were introduced in the previous section, with the extended Prout-Tompkins (ePT) and Avrami-Erofe'ev equations as two examples. In fact, the variations are far more extensive. The first appearances of these equations were actually prior to the papers from which they are commonly named.

An introduction to the various nucleation-growth models in the solid state literature is given by Brown et al. [61]. The simplest nucleation-growth model does not recognize the overlapping consumption of reactants and leads to the power law in Table 2.1. Avrami [62], Johnson and Mehl [63], and Kolmogorov [64] and Erofe'ev [65] then independently considered the merging of reaction centers, obtaining

$$\alpha = 1 - \exp(-kt^p). \tag{2.30}$$

This equation is known variously as the Avrami equation, the JMA equation, the JMAK, and the JMAEK equation after its originators. It assumes that the reaction nucleates (initiates) randomly and homogeneously over the entire unconverted volume and grows uniformly in all directions. Solving for kt, it is evident that this equation is the $g(\alpha)$ given in Table 2.1. The value of p was once considered to be the sum of the number of steps in the nucleation process and number of growth dimensions, but it is now generally treated only as an empirical constant.

Prout and Tompkins [66] used a different approach to model the thermal decomposition of potassium permanganate. They found that the decomposition followed the logistic equation

$$\ln\left[\frac{\alpha}{1-\alpha}\right] = kt + c, \tag{2.31}$$

which corresponds to the rate form

$$\mathrm{d}\alpha/\mathrm{d}t = k(1-\alpha)\alpha. \tag{2.32}$$

The Prout-Tompkins model is more closely related to autocatalytic reactions than nucleation-growth reactions with overlapping volumes [67].

Šesták and Berggren [68] proposed an empirical equation that combines aspects of the Prout-Tompkins and JMAEK equations:

$$d\alpha/dt = k\alpha^m(1-\alpha)^n[-\ln(1-\alpha)]^s. \tag{2.33}$$

This equation has all the limits of the *n*th-order, ePT, and Avrami-Erofe'ev (JMAEK) models, although s in this equation equals $1 - 1/p$ in the Avrami equations in Table 2.1.

What my coworkers and I call the ePT model ($s = 0$ in Eq. 2.33) has an interesting history. Although the name for this class of models comes from the 1944 paper of Prout and Tompkins on decomposition of $KMnO_4$, it actually appears earlier in the literature. Austin and Rickett [69] considered both the normal autocatalytic equation (Eq. 2.31) and the logarithmic analog

$$\ln[\alpha/(1-\alpha)] = k\ln t + c, \tag{2.34}$$

for analyzing decomposition kinetics of austenite, an allotrope of iron or steel. The latter worked better for them, and Prout and Tompkins [70] also found in a later paper that the logarithmic form worked better for $AgMnO_4$. Avrami refers to the Austin and Rickett paper part I of his series [62] as a limit of his equation, and Erofe'ev [71] showed by series expansion and grouping that ePT model is equivalent with the Avrami-Erofe'ev (JMAEK) model with certain ordered pairs of n and m. A more extensive numerical comparison appeared recently [72]. Finally, the ePT model (n and $m \neq 1$) actually appears in a 1940 Russian publication [73] that only recently has been recognized in the English literature [60].

More recently, a generalized form of the logistic equation [74, 75] was introduced to chemical kinetics analysis:

$$1 - \alpha = 1/(1 + \tau e^{-b(t-c)})^{1/\tau} \tag{2.35}$$

where b is a reaction rate parameter, t is either time or temperature, and c is the midpoint of the reaction in either time or temperature for a constant heating rate. (Note in contrast that c in Eq. 2.31 is dimensionless.) When differentiated this equation gives

$$d\alpha/dt = -be^{-b(t-c)}/(1 + \tau e^{-b(t-c)})^{\frac{1}{\tau}+1} \tag{2.36}$$

Comparing Eqs. (2.35) and (2.36) to Eqs. (2.31) and (2.32), respectively, indicates that if t is time, c is an arbitrary shift in time, b is the negative of the conventional rate constant, and τ is a new shape parameter. Numerical studies [76] show that the parameter τ has basically the same effect as reaction order in the ePT model, with $\tau = 0.1$ comparable to $n = 1.7$ and $\tau = 3.0$ comparable to $n = 0.65$. Although the implementation of the generalized logistic equation by that group is not optimal and is less flexible than the ePT model, it is a potentially useful method if properly implemented.

An issue with some simple forms of sigmoidal reaction models is that the initial reaction rate is zero and the reaction can never begin. This can be rectified in several ways, but it is very instructive to first explore one more complete version of an autocatalytic model commonly used for energetic materials [10]. Consider the reaction sequence

$$\mathbf{A} \rightarrow \mathbf{B};\ \mathbf{B} + \mathbf{A} \rightarrow 2\mathbf{B}$$

which can be described mathematically by the relation $d\mathbf{A}/dt = -k_1\mathbf{A} - k_2\mathbf{AB}$. The differential equation cast in terms of fraction reacted in the thermal analysis style is

$$d\alpha/dt = k_1(1-\alpha)^{n1} + k_2\alpha^m(1-\alpha)^{n2}. \tag{2.37}$$

The empirical reaction orders are added for flexibility. If we assume that $n_1 = n_2$, then

$$d\alpha/dt = k_2(1-\alpha)^n(\alpha^m + z) \approx k_2(1-\alpha)^n[1-q(1-\alpha)]^m \tag{2.38}$$

where $z = k_1/k_2 \approx 1 - q$. The left-hand approximation is used in CISP software [77], and the right-hand approximation is used in Kinetics2015. The z and q factors are basically ways of starting numerical integration with a non-zero reaction rate in the absence of an explicit initiation reaction, and they can be optimized to fit any data set. While no analytical solution is available for these equations, a solution is available for n and m equal to 1 (basic Prout-Tompkins limit):

$$\alpha = 1/(e^{-kt}(1-\alpha_0)/\alpha_0 + 1) \tag{2.39}$$

where α_0 is the integration constant that provides an initial fraction reacted to start the reaction.

Brown et al. [78] observe that it is difficult to distinguish whether the ePT or JMAEK approaches fit any given data set better. That has been my experience, also, so I have used the ePT approach almost exclusively. A qualitative comparison [79] of the two approaches is reproduced in Fig. 2.5. The two models could be matched even closer by optimizing the factor q if desired.

A further comparison of the logarithmic (Eq. 2.34) and ePT approaches is also instructive. (Recall that Prout and Tompkins found that $AgMnO_4$ was sigmoidal in logarithmic time while $KMnO_4$ was sigmoidal in linear time.) A conversion versus time curve was generated using Eq. (2.34) solved for α and then fitted by nonlinear regression to the right-hand approximation of Eq. (2.34). The results are shown in Fig. 2.6. There is a hint of an acceleratory phase when plotted on a linear scale, but the sigmoidal character is clearly evident on a logarithmic scale. The agreement is as good as needed for any practical purpose.

In discussions with researchers doing pyrolysis of cellulose and kerogens, some resisted the adoption of a sigmoidal reaction model despite clear evidence that it was necessary. One doubted that models developed for inorganic materials were

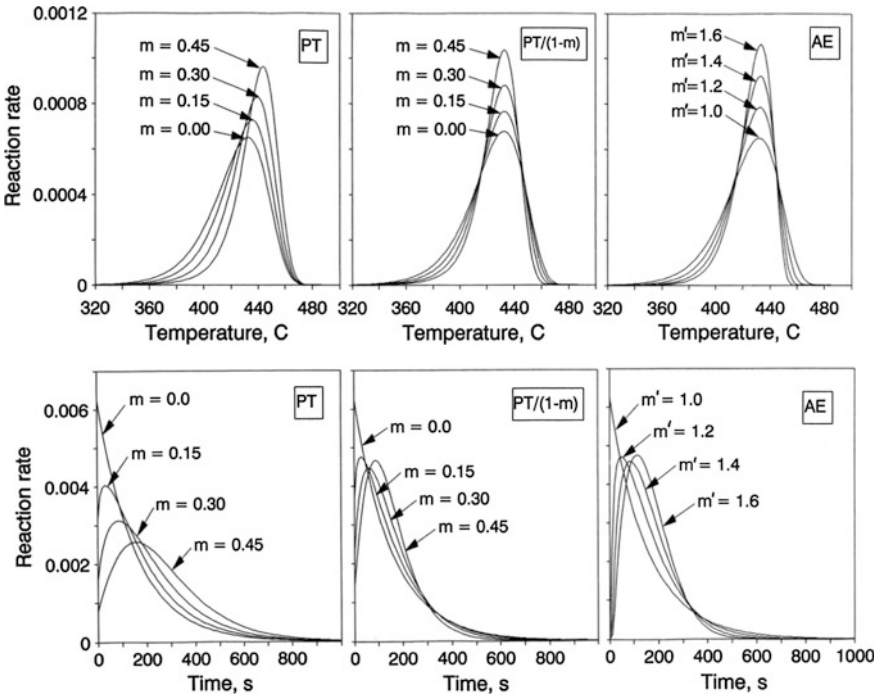

Fig. 2.5 Comparison of extended Prout-Tompkins and Avrami-Erofe'ev approaches to modeling acceleratory reaction rates from Burnham et al. [79]. The ePT calculations used $q = 0.99$, and the frequency factor had to be renormalized by $1/(1 - m)$ for T_{max} to be independent of m. The symbol m' was used in the Avrami equation in that paper instead of the symbol p in Table 2.1. Reproduced courtesy of LLNL

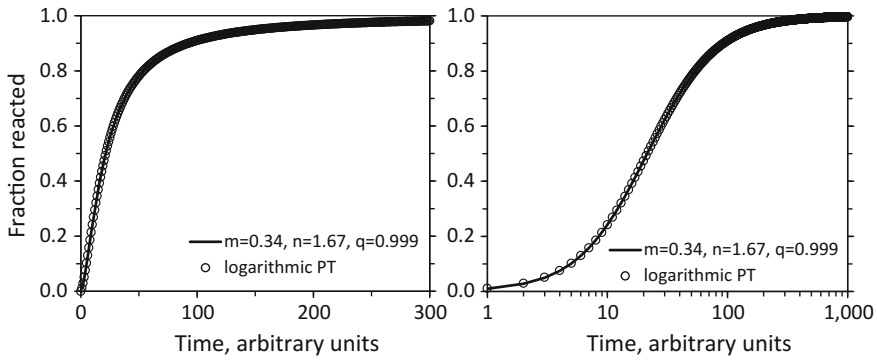

Fig. 2.6 Demonstration of the ability of the ePT model to fit logarithmic sigmoidal reaction characteristics [76]. © Springer

relevant to organic pyrolysis. Another thought it was fine to allow the frequency factor to depend on heating rate and thereby increase the activation energy to narrow the reaction profile enough to match experiment. Both positions are without merit. The following paragraphs give published examples to support that statement.

It has been known for a 100 years or so that organic pyrolysis reactions occur by chain reactions. By the early 1930s, detailed mechanisms [80] had been worked out for initiation, propagation, and termination of hydrocarbon cracking, including how to calculate the overall activation energy from the activation energies of the various steps.

The essence of a chain reaction is that there is an active center that initiates the chain, a chain propagation step that generates some number of new active centers, and a quenching reaction that ends the chain. Although the chemical and physical processes of each step may differ, the mathematics is the same unless one develops a detailed mechanistic model, which is beyond the objectives of this book.

The most directly relevant analog to kerogen pyrolysis comes from synthetic polymer pyrolysis, which was explored in great detail about 50 years ago. Flynn and Florin give [81] a good review of that work, including a lengthy report from the National Bureau of Standards and multiple books. They summarize the main mechanisms as random main-chain scission, depolymerization, side-group reactions, and carbonization.

Random chain scission is the breaking of the main chain to form smaller molecules of all sizes. The molecular weight falls, eventually forming molecules small enough to be volatile. There is no preference for monomer formation. For example, polyethylene and polypropylene decomposition do not preferentially form ethylene and propylene. Depolymerization is the unzipping of the polymer after an occasional break. Monomer formation is primary. Tetrafluoroethylene, α-methyl styrene, and methyl methacrylate are examples. Side-group reactions involve the elimination of a labile group off the main chain. Examples include elimination of hydrogen chloride from polyvinyl chloride to leave a polyene structure and elimination of isobutylene from poly(*t*-butyl methacrylate) to leave polyacrylic acid.

Carbonization is the formation of a carbonaceous residue and involves a variety of processes, usually in parallel with random scission. It may include cross-linking, polyene formation by elimination of side chains, cyclization, and aromatization of cyclics. In the coal literature, "retrograde reactions" is sometimes used as a descriptor. Lyon et al. [82] deduced group formation contributions to char formation and found that poly-aromatic-heterocyclic rings were the strongest char former, while simple aromatic groups were far less char-prone—e.g., polystyrene forms little char. Formation of carbon fibers from polyacrylonitrile involves cyclization of the nitrile side chains and aromatization, enhanced by mild oxidation.

Flynn and Florin [81] review depolymerization theory and present theoretical results for various situations. Depending on the initiation location and unzipping length in the absence of chain transfer, the reaction rate versus conversion can be either deceleratory or autocatalytic, as shown in Fig. 2.7, which is adapted from Wall [83]. Note that the end initiation with small unzipping length leads to a flat reaction curve, because each end is generates volatiles at a constant rate and the

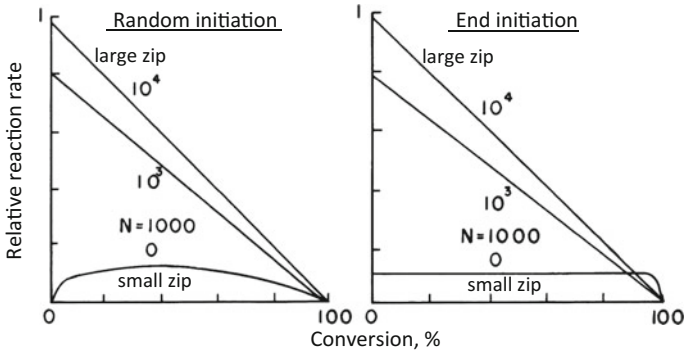

Fig. 2.7 Theoretical calculations of the depolymerization reaction rate versus conversion for various assumptions of initiation location and unzipping lengths (zip). Adapted from Wall [83] with permission. © 1962 Wiley Interscience

number of ends remains constant until most of the material is consumed. In contrast, random initiation with a small unzipping length results in an acceleratory phase, as the number of ends generating volatiles increases with time during the first phase of pyrolysis. For very large unzipping lengths, the overall rate decreases with time, because a single initiation consumes the entire chain and the number of chains decreases with time.

Flynn and Florin [81] then review random scission theory and, as noted previously by Burnham et al. [10], summarize equations that have similar functional form to the Prout-Tompkins model. As shown by Flynn and Florin for polyethylene and in the original work by Wall and Straus [84] for a wider range of polyolefins (see Fig. 2.8 for the polyethylene example), the rate of devolatilization is always autocatalytic in shape (sigmoidal in fraction reacted) for linear polyolefins but strictly deceleratory for branched polyolefins. This is because the probability of

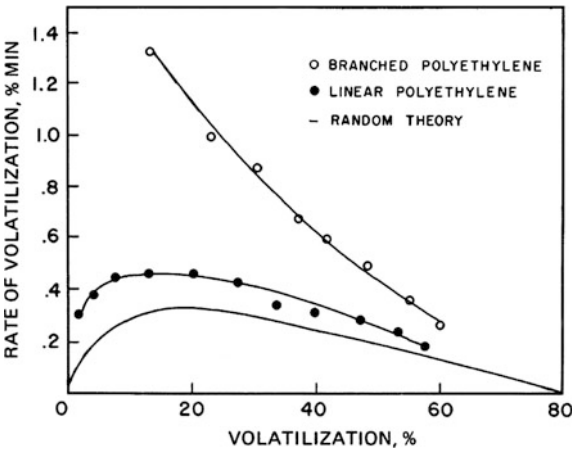

Fig. 2.8 Effect of chain branching on volatilization rate versus conversion for polyethylene pyrolysis at constant temperature, adapted from Wall and Straus [84]. Reprinted with permission. © 1960 Wiley

generating a volatile fragment for a given scission is proportional to the amount of material present for a branched material, while random scission of linear material generates primarily shorter, non-volatile chains initially. As the chains get shorter, the probability of a volatile product from a given scission increases with time until the amount of material has decreased enough that the rate becomes deceleratory.

After success fitting a variety of kerogen samples with first-order and distributed activation energy models, my first measurements of polymer pyrolysis provided a rude awakening—the reaction profiles of several of the polymers provided by a colleague, Richard Lyon, were narrower than could be calculated by a first-order model using an activation energy derived by Kissinger's method [85]. Using a reaction order less than one matched the profile width but didn't get the shape right. We noticed the same character for one kerogen sample, and we correlated the characteristic of a narrow reaction profile with an acceleratory phase during isothermal pyrolysis [86].

It was another 6 years before these characteristics were fully connected to the polymer and solid state kinetic model literature [79]. During that time, we found that a sequential reaction gave fits comparable to the nucleation-growth approach, but the non-linear regression was not as robust. Consequently, from the practical perspective of this book, there is little reason to explore models other than the ePT model. A few examples of its utility for polymers follow.

Prior publications [4, 87, 88] showed that polyethylene, poly(1,4-dimethylene naphthalene), polystyrene, polysulfone, polycarbonate, polyether-ether-ketone (PEEK), Kel-F 800, and Viton-A have essentially single decomposition reactions that are narrower than predicted from first-order kinetic parameters derived from Kissinger's equation. The ratio of measured to calculated profile widths ranged from 0.36 to 0.86, with an average of 0.62. At the same time, the peak shapes were different, with asymmetry factors ranging from 0.6 (slightly less asymmetric than a first-order reaction) to 1.1 (skewed to high temperature significantly more than a first-order reaction. In addition, two polymers with two clear decomposition steps, Estane and poly(vinyl acetate), had one of the two steps being narrower than a first-order reaction. The resulting ePT model parameters for these polymers ranged from 0.23 to 0.90 for m, with an average value of 0.62, and from 1.0 to 2.2 for n, with an average value of 1.3. Comparing these averages to the parameters in Fig. 2.6, linear polymers are generally between the linear and logarithmic forms of the Prout-Tompkins model.

A recurring question in the literature is whether kinetics derived from constant heating rate experiments agree with those derived from isothermal experiments. If the kinetic model is correct, they should and can agree. Such agreement is shown in Fig. 2.9 for the decomposition of PEEK [89]. In this case, the kinetic model was optimized simultaneously on the heating rate and isothermal data. For three other cases [88], the ePT kinetic model was calibrated on heating rate data and then compared with isothermal data. The agreement was not as close but was qualitatively correct. Kel-F showed the poorest agreement of the three polymers, as shown in the left side of Fig. 2.10. A refit of the Kel-F data to both constant heating rate and temperature data is shown in the right side of Fig. 2.10. The agreement with the

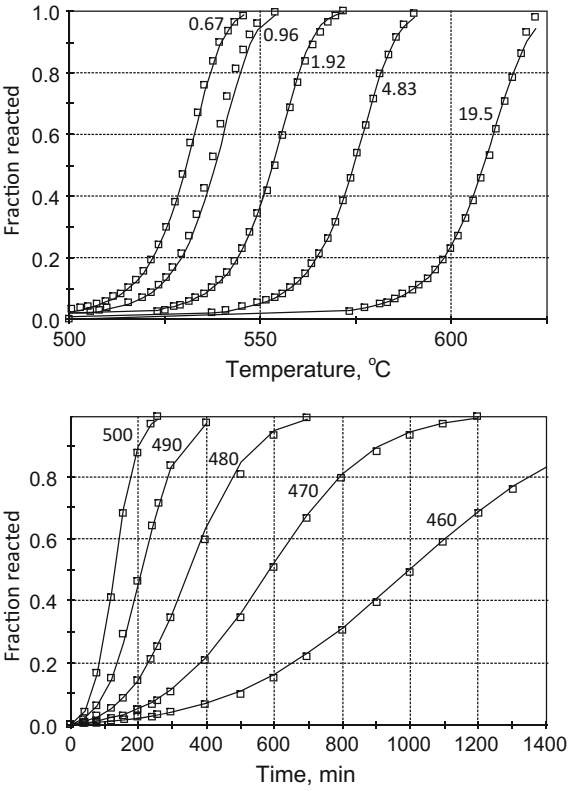

Fig. 2.9 Fit of the ePT model to PEEK decomposition data from Nam and Sefaris [89]. The indicated heating rates are in °C/min and the temperatures are in °C. The kinetic parameters are $A = 2.4 \times 10^{14}$ s^{-1}, E/R = 28,940 K, m = 0.86, and n = 0.89. Reproduced courtesy of LLNL

isothermal data is better, as would be expected, but the fit to the constant heating-rate data is not as good. E/R changes from 15,450 to 13,217 K. The isothermal data was taken 2 years after the constant heating rate data, so it is an open question whether the discrepancy is an experimental or model problem. This example shows the importance of fitting a diverse set of thermal histories to be sure one has the correct model and model parameters. We return to this issue later in Sect. 2.7 on how to select a model to fit.

Cellulose also has a narrow reaction profile and acceleratory phase, and consequently requires a sigmoidal reaction model [2, 90, 91]. The ePT growth parameter m was between 0.4 and 0.5 for three different samples, and activation energies were in the mid 40 kcal/mol range. These results are qualitatively consistent with earlier work by Dollimore and Holt [92] that showed an acceleratory phase on a reduced time plot, from which they concluded that a nucleation-growth model was most appropriate and that the data was consistent with an Avrami exponent p of 2. That corresponds to $m \approx 0.75$ according to an extrapolation of Fig. 2.5.

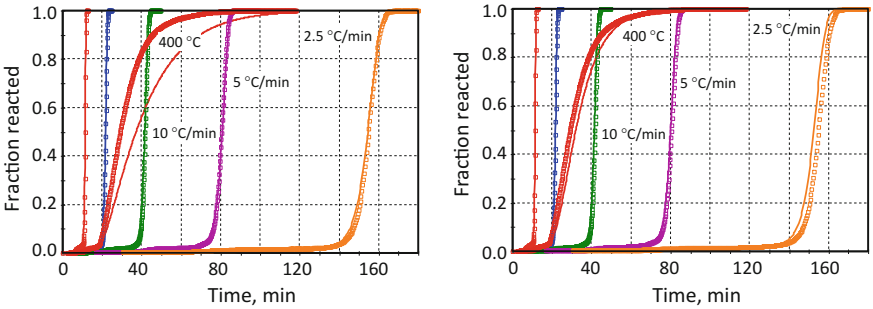

Fig. 2.10 Fit of the ePT model to Kel-F decomposition data from Burnham and Weese [88]. Heating rates were 2.5, 5, 10, 20 and 40 °C/min. The *left figure* shows a fit to the heating-rate data only with a comparison to the 400 °C isothermal data. The *right figure* shows a fit to all data

During this time period, a leader in the biomass community recommended against the publication of Reynolds and Burnham [90] because he believed cellulose pyrolysis was first order. He subsequently led a round robin exercise that fitted a first-order model independently to pyrolysis data at two different heating rates [93], in direct conflict with the conclusions in Reynolds and Burnham [90] and the best practices outlined in the two subsequent ICTAC papers on kinetic analysis [6, 38]. The eight independent measurements of T_{max} from different labs give a fairly reliable estimate of the average T_{max} value, and A and E calculated from Kissinger's method are $A = 1.75 \times 10^{15}$ s^{-1} and 48.04 kcal/mol, in excellent agreement with Capart et al. [91]. In contrast, the average activation energies from single heating rate fits were 58.32 and 53.06 kcal/mol, respectively, at 5 and 40 °C/min, which do not make chemical sense in terms of the bond strengths.

All of the first-order Arrhenius parameter pairs derived in the round robin are plotted in a compensation-law plot in Fig. 2.11 [94]. They fall on a line with the parameters from Kissinger's method. Calculating the average profile widths from the round robin and Kissinger method kinetics, one finds that the measured pyrolysis profile is only 84 % of the first-order width. That corresponds to a value of m of about 0.3, which is qualitatively consistent with Capart et al. [91].

Fortunately, others in the cellulose pyrolysis field eventually understood the need for a sigmoidal reaction model. Kim and Eom [95] used TGA and reduced-time plots to choose a reaction model and determine an Avrami exponent of 3.7, which is highly acceleratory. Barud et al. [96] used a nonlinear isoconversional approach to confirm that cellulose pyrolysis followed the Avrami-Erofe'ev model with an exponent p of 1.63 and an activation energy of about 44 kcal/mol. The Avrami exponent corresponds to an ePT value for m of 0.45. These parameters are very close to those of Reynolds-Burnham. Similarly, Sanchez-Jimenez et al. [97] used a master plot approach discussed further in a following section to show that the appropriate

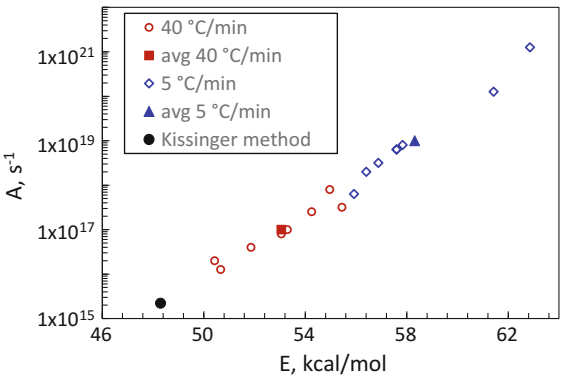

Fig. 2.11 Arrhenius parameters determined in a round robin study of cellulose pyrolysis [93]

model was either a random-scission kinetic model mathematically similar to the ePT model or an Avrami-Erofe'ev model with $p < 1.5$. Figure 2.5 puts their equivalent m value for the ePT model at ~ 0.4, and their activation energy of 46 kcal/mol is between those of Capart et al. and Reynolds-Burnham. Ultimately, comparison of global kinetic modeling to mechanistic modeling showed that cellulose pyrolysis is not first order but is consistent with a random-scission or nucleation-growth model [94]. Even so, there are still questions about how much of the sigmoidal character is due to the chemical reaction mechanism and how much is due to delayed vaporization of pyrolysis products, but that does not excuse the practice of fitting a single heating-rate experiment to a first-order reaction model.

The lesson here is that leaders in a field are sometimes slow to believe and adopt the obvious need to move on from commonly used historical pyrolysis models. We will also see that in the kerogen pyrolysis literature.

2.6 Distributed Reactivity Models

The concept that a complex reaction proceeds by a distribution of independent parallel reactions is very old, dating back at least to 1925 to the work of Constable, who noticed a compensation effect between A and E for surface catalyzed reactions and proposed that the surface had a variety of sites that led to a distribution of activation energies governing the reaction [98]. In 1943, Vand [41] developed a reactivity distribution model for irreversible electrical resistance changes upon annealing of evaporated metal films. The parallel reaction approach got greater exposure from the work of Pitt [99] and Hanbaba [100] in the coal pyrolysis community in the 1960s. Probably the next influential step was the Gaussian energy distribution model popularized by Anthony and Howard [13] for coal pyrolysis,

which continues to be common today despite its shortcomings. Finally, workers at the Institut Français du Pétrole developed the discrete energy distribution model for petroleum generation, and the first version having reasonable kinetic properties was published by Ungerer and Pelet [101]. A concurrent approach to reactivity distributions originates from the isoconversional methods of Friedman [29] and Ozawa [30], which were originally designed for determining a single activation energy and reaction order but have been used more often to determine how the activation energy varies with conversion. A variety of other historical developments are described by Burnham and Braun [4].

The distributed reactivity models all have their basis in Eq. (2.7). To generalize to an arbitrary number of parallel reaction channels, we first define x_i as the fraction remaining of the ith reaction potential, giving

$$1 = x_0 = \sum\nolimits_i a_i x_{i0}; \sum\nolimits_i a_i = 1; x(\mathrm{t}) = \sum\nolimits_i a_i x_i(t) \tag{2.40}$$

Differentiating the right-hand equation yields

$$\frac{dx}{dt} = \sum\nolimits_i a_i \frac{dx_i}{dt} = \sum\nolimits_i a_i k_i(T) f(1 - x_i), \tag{2.41}$$

which is an explicit summation of Eq. (2.7), where the $f(1 - x_i)$ are given in Table 2.1. Obviously, Eq. (2.41) can be used in this discrete summation for any reaction for which $f(1 - x_i)$ is known. Now consider replacing the discrete sum with a continuous mathematical distribution, but restrict the derivation to a first-order reaction, for which the integration over any thermal history is given in Eq. (2.9). If the distribution in reactivity is given by a distribution in activation energy only,

$$x = \int_0^\infty \exp\left[-\int_0^t k(T(t))dt\right] D(E)dE \tag{2.42}$$

and

$$\int_0^\infty D(E)dE = 1. \tag{2.43}$$

Two commonly used distributions are the Gaussian distribution:

$$D(E) = (2\pi)^{1/2}\sigma^{-1} exp\left[-(E - E_0)^2/2\sigma^2\right] \tag{2.44}$$

where σ is the normal distribution parameter, and the Weibull distribution:

$$D(E) = \frac{\beta}{\eta}\left[\frac{(E-\gamma)^2}{\eta}\right]^{\beta-1} \exp\left\{-\left[\frac{(E-\gamma)^2}{\eta}\right]^{\beta}\right\} \tag{2.45}$$

where η is a width parameter, β is a shape parameter (not the heating rate in this section), and γ is the activation energy threshold. The mean activation energy is given by

$$E_0 = \gamma + \eta\Gamma\left(\frac{1}{\beta} + 1\right) \tag{2.46}$$

where $\Gamma()$ is the Gamma function. The Weibull distribution is much more flexible, being able to change in both shape and width, but only a few workers (as described by Burnham and Braun [4]) have explored its use.

Burnham and Braun [4] provide a variety of comparisons between various activation energy distribution models. As the Weibull distribution parameter η increases, so do the values of σ and n when simulated Weibull data are fitted to a Gaussian distribution or nth-order reaction model. A Weibull energy distribution having $\eta = 3$ and $\beta = 1$ corresponds very closely to an nth-order reaction with $n = 2.7$. Any number of such comparisons could be constructed.

It is important to understand that a distribution in activation energy is not the only way to introduce a reactivity distribution. From a different perspective, Kolar-Anić and Veljković [102] explored the use of Gamma and Weibull distributions of reactivity to understand the Avrami exponent p in a variety of systems. Ho and Aris [103] show that a Gamma distribution of rate constants for isothermal conditions leads to apparent nth-order kinetics, with second order corresponding to the limit of an exponential distribution of reactivity, which at isothermal conditions is equivalent to a distribution of pre-exponential factors. Burnham and Braun [4] use that concept to justify nth-order kinetics in combination with a Gaussian distribution of activation energies to gain the shape flexibility of a Weibull distribution, at least to the extent that it is needed to model pyrolysis reactions, and that approach was quite useful for modeling the process of sintering [104].

It is also important to understand that a distribution in reactivity is not the same as using a logistical distribution function to fit reaction profile shapes, as was done by Cai and Liu [105]. While the latter might be a useful method for preprocessing reaction profiles to eliminate noise, it does not result in fundamental kinetic parameters that can be used for modeling conditions other than those fitted.

Some have looked for analytical equations to simplify the use of continuous reactivity distributions for specific situations, e.g., a Gaussian energy model for a constant heating rate [106], but we have found it more practical to break any continuous distribution of activation energy into a discrete distribution of evenly spaced energies. The reason is twofold. First, we find the numerical integration of independent parallel first- and nth-order reactions is quite fast compared to having to evaluate complex exponential functions. Second, we prefer to write software for arbitrary thermal histories, because experimental data and industrial applications rarely follow the ideal thermal histories people usually analyze.

One must consider how the energy spacing between reaction channels affects the validity of the model. Our original work [23] used 0.25 kcal/mol spacing, but subsequent numerical studies found that 0.5 kcal/mol spacing was adequate. For

systems that are characteristically broad in terms of reactivity distribution, using *n*th-order reactions with $n = 1.5$ (approximately symmetrical for a constant heating rate) or 2.0 (skewed to high temperature) in the distribution allows one to cut the number of reaction channels by 1.5–2 times without compromising accuracy, thereby speeding computational time. Furthermore, an *n*th-order model with $n = 1.001$ is insignificantly different from a true first-order model, so programming only one type of reaction would be required for each reaction channel. If not needed to adjust the reaction peak shape, one could have the reaction order change in concert with the energy distribution width in some predetermined manner to minimize the additional channels needed for a wide reactivity distribution.

In a complex material such as a fossil fuel, different products are evolved at different stages of maturity, so it is likely that a simple mathematical distribution will not have flexibility to fit the reaction profile of some reactions. Discrete activation energy distributions were developed to provide that flexibility. Initially, the model had a single pre-exponential factor and weighted first-order reaction channels placed at discrete intervals. The first implementation by the IFP [101] used 20 channels spaced at 2 kcal/mol from 40 to 80 kcal/mol and optimized the pre-exponential factor and weighting factors by nonlinear regression. We subsequently developed [106] a much faster, iterative constrained linear/nonlinear regression method for the same optimization, including algorithms to select the correct number of reaction channels constrained by the data and a user-selected channel spacing, which we recommended to be 1 kcal/mol for most materials. This general approach is the most commonly used method in the petroleum exploration geochemistry community.

The additional flexibility of the discrete model compared to a single distribution model enables it to easily fit the reaction profiles of coal and other materials that have multiple overlapping chemical reactions. Neither the Weibull nor the *n*th-order Gaussian models were able to simultaneously fit the relative sharp profile from 10 to 80 % conversion and the broader reaction profiles for the initial 10 % and final 20 % of the reaction, as shown in Fig. 2.12. Although fitting three parallel Weibull or Gaussian-*n*th models could do considerably better than a single such model, the discrete model fits the profiles with ease.

An issue that has been explored at some length is the proper energy spacing between reaction channels. Recall that we found that 0.5 kcal/mol spacing was adequate to discretize an analytical distribution with negligible error. Increasing the reaction channel spacing to 1 kcal/mol still introduces negligible error compared to the limitations of an analytical form. The discrete model optimization is a little different, in that too wide of a spacing causes a modulation of the minimization function corresponding to shifting the distribution by the channel spacing and compensating with a change in the optimum pre-exponential factor. This is shown in Fig. 2.13, which is reproduced from Sundararaman et al. [107]. Clearly, when most of the reaction occurs in one reaction channel, the energy spacing must be less than 1 kcal/mol to be sure of a good optimization, and Kinetics2015 allows them to be 0.5 kcal/mol. Second, when the reactivity spans an activation energy range of several kcal/mol, 1 kcal/mol spacing is needed.

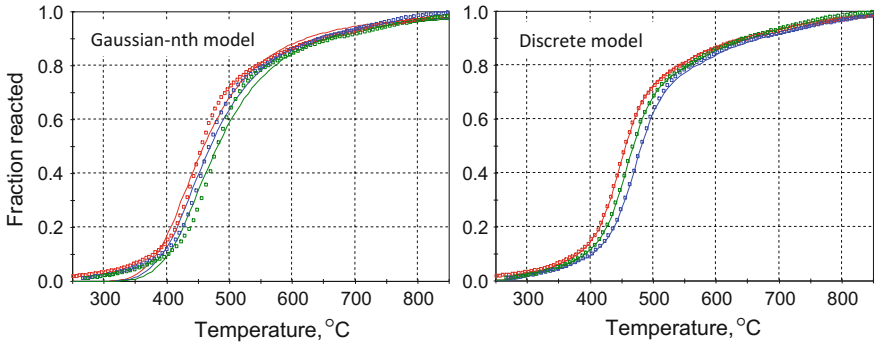

Fig. 2.12 Comparison of the ability of the *n*th-order Gaussian distribution and discrete distribution models to fit coal pyrolysis data at 5, 10, and 20 °C/min. A Weibull distribution fit was comparable to the Gaussian-*n*th fit

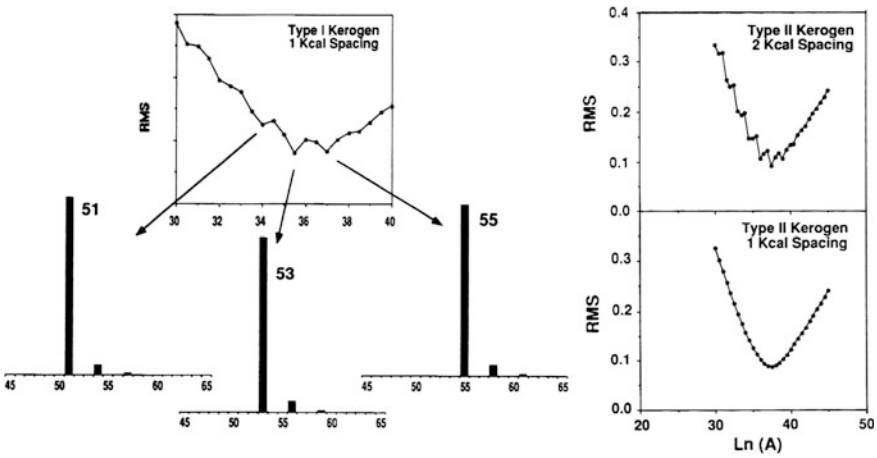

Fig. 2.13 Graphics from Sundararaman et al. [107] showing the effect of too-widely-spaced energy channels on the nonlinear regression minimization surface and the probability of finding a false minimum. *RMS* = Root-mean-squared deviation. Reprinted with permission. © 1977 American Chemical Society

Kinetics2015 allows the user to pick a larger spacing, and the program improves the probability of finding the right minimum even if the user chooses too large of spacing by using the characteristics of the compensation law. The minima are spaced by the relationship that a 1 kcal/mol shift in the activation energy distribution is compensated by a factor-of-two change in the pre-exponential factor. Once a minimum is found, Kinetics2015 searches on both sides of the minimum by that spacing to assure that the correct minimum is found.

A second important issue is whether it is appropriate to assume the same pre-exponential factor for all energy channels. Such an assumption simplifies

programming of industrial applications, but it is certainly not necessary. It is possible, and Kinetics2015 allows the pre-exponential factor to be a linear function of the activation energy, which is consistent with the concept of a compensation law that is a function of the chemical reactions and not merely a reflection of experimental error.

The effect of such a compensation relationship is to spread the activation energies over a wider range, which may or may not be chemically realistic [4]. As a result, an extrapolation outside the temperature range of calibration will spread the reaction over a wider temperature range. Such an example is given in Fig. 2.14, which is calculated from kinetic parameters in Table 9 of Burnham and Braun [4]. Whether or not the variable *A* kinetics are more correct, the difference in predictions is not too large, and it is doubtful that it would make a difference in any exploration drilling decision given all the other uncertainties in paleo thermal history reconstruction. Consequently, there has been no compelling reason for those involved in oil and gas exploration to incorporate the complication of a variable *A* into their petroleum generation calculations, and it is rarely, if ever, done.

Isoconversional methods were originally envisioned to determine a best single activation energy, but they are currently used more to determine the dependence of activation energy on conversion. The Friedman model does that without approximation, but all integral isoconversional methods except the advanced integral model of Vyazovkin [37] assume that the activation energy is constant up to the point of analysis, which is self-contradictory, and Vyazovkin's method obtains values essentially the same as Friedman's method.

There are two philosophies on how to deal with a distribution of activation energies from isoconversional methods. One is to consider that the activation energy at the *i*th conversion point is simply the average activation energy at that conversion. However, Miura [39, 40] argues that reaction profiles are not delta functions, so any given level conversion involves overlapping of reactions with different activation energies. He then derives a relationship for the effective boundary between energies that have and have not significantly contributed to the conversion to that point. Next, he replaces the equation

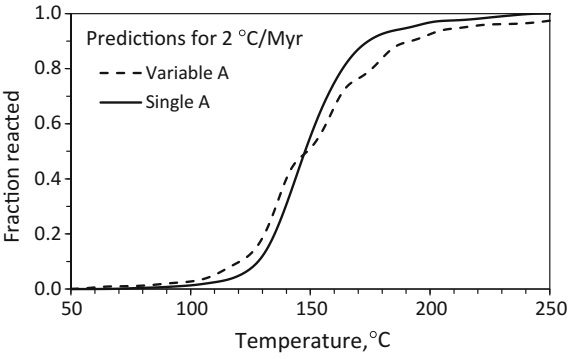

Fig. 2.14 Predictions of oil and gas generation from a Ventura Basin Monterey shale sample using discrete activation energy models with a single and variable pre-exponential factor (Myr = million years)

$$x = \exp\left[-\frac{ART^2}{\beta E} e^{-\frac{E}{RT}}\right] \tag{2.47}$$

(which drops all the series-expansion terms in Eq. 2.14) by the equation

$$x = \exp\left[-\frac{0.545ART^2}{\beta E_s} e^{-\frac{E_s}{RT}}\right]. \tag{2.48}$$

He then calculates A and E pairs by an isoconversional method so that the measured and calculated reaction curves agree.

Cai et al. [108] criticize Miura's method by saying that it does not recover a constant frequency factor when simulated data from Gaussian distribution models using a constant frequency factor are fitted to Miura's method. In fact, that characteristic was pointed out far earlier by Burnham and Braun [4], and Friedman's method has a similar characteristic. However, one should realize that the derived parameters compensate for each other in a way mandated by the mathematics, and the real issue is how well they work for thermal histories besides those used for calibration. In that respect, both the Friedman and Miura methods work adequately, as shown by Burnham and Braun. Which method to use is a matter of personal taste.

Miura [40] presents A-E distributions determined in this way for the Argonne premium coals. Burnham and Braun [4] found good correspondence between those distributions those determined by the extended discrete model in Kinetics2015. Whether it provides a practical advantage over Friedman's method or merely provides an alternative way to define the effective activation energy at any extent of conversion is another matter.

Some insights on these issues are provided by the following example. Simulated data at 1.0 and 10 °C/min were created using a parallel reaction model having the properties in Table 2.2. The simulated data were fitted to two different discrete parallel reaction models: one having a single A factor and one where A depends on activation energy. The results of those fits are also given in Table 2.2. Despite, the fewer number of parameters in the extended discrete model ($\ln(A) = a + bE$), it fits the data significantly better, as shown in Fig. 2.15. The reaction rates rather than fraction reacted are shown because they are more sensitive to the quality of the fit. Both fits recover the properties principal reaction channel quite well.

Isoconversional analysis by Friedman's method yields the parameters shown in Fig. 2.16. They are closely related to but not identical to the input model parameters, in large part because of the fundamental differences in the nature of the models themselves. Friedman's method recovers the parameters for the effective mix of reactions at any conversion level, while the discrete model deconvolves that overlap. If one wants to compare activation energy distributions from isoconversional analysis to a parallel reaction model, one must do something along the lines of Miura's analysis. Good correspondence was shown earlier [4], but it is not obvious that such a comparison is warranted for ordinary purposes.

Table 2.2 Input and derived parallel reaction models having discrete distributions of activation energies, one with a single A and one where A depends on E

Input model			Extended discrete model fit			Ordinary discrete model fit		
%	A, s^{-1}	E, cal/mol	%	A, s^{-1}	E, cal/mol	%	A, s^{-1}	E, cal/mol
1	1×10^{12}	40,000				0.01	1.88×10^{18}	51,000
2	1×10^{13}	44,000	2.06	1.18×10^{13}	43,093	0.01	1.88×10^{18}	52,000
4	1×10^{14}	48,000				0.03	1.88×10^{18}	53,000
6	1×10^{15}	52,000	7.12	4.87×10^{14}	49,943	0.07	1.88×10^{18}	54,000
8	1×10^{16}	56,000				0.15	1.88×10^{18}	55,000
16	1×10^{17}	60,000	17.61	2.01×10^{16}	56,794	0.37	1.88×10^{18}	56,000
26	1×10^{18}	64,000	44.45	8.32×10^{17}	63,644	0.66	1.88×10^{18}	57,000
16	1×10^{19}	68,000	20.49	3.44×10^{19}	70,495	1.08	1.88×10^{18}	58,000
8	1×10^{20}	72,000				1.64	1.88×10^{18}	59,000
6	1×10^{21}	76,000	7.23	1.42×10^{21}	77,345	2.62	1.88×10^{18}	60,000
4	1×10^{22}	80,000				3.74	1.88×10^{18}	61,000
2	1×10^{23}	84,000	1.04	5.87×10^{22}	84,195	5.44	1.88×10^{18}	62,000
1	1×10^{24}	88,000				7.76	1.88×10^{18}	63,000
						16.84	1.88×10^{18}	64,000
						27.44	1.88×10^{18}	65,000
						14.99	1.88×10^{18}	66,000
						9.15	1.88×10^{18}	67,000
						7.04	1.88×10^{18}	68,000
						0.8	1.88×10^{18}	69,000
						0.12	1.88×10^{18}	70,000
						0.04	1.88×10^{18}	71,000

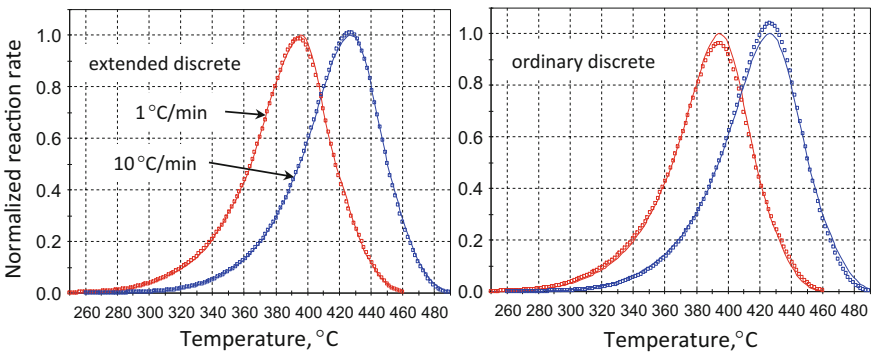

Fig. 2.15 Comparison of the extended and ordinary discrete model fits (*lines*) to simulated data (*points*) at 1 and 10 °C/min. The ordinary discrete model has a single pre-exponential factor, and the extended discrete model has one that depends on activation energy

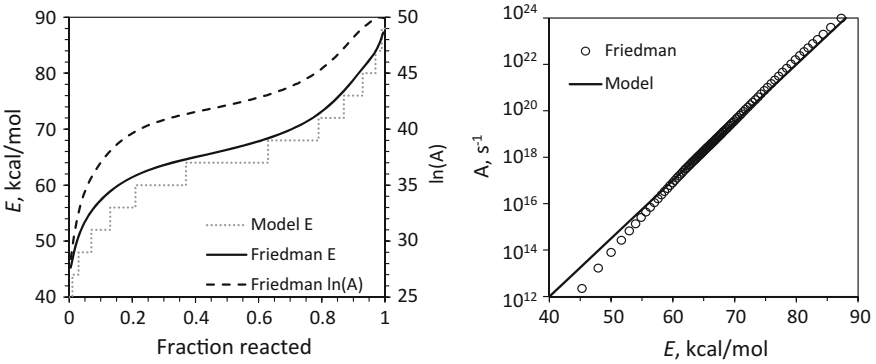

Fig. 2.16 Comparison of isoconversional kinetic parameters with the input model parameters used to generate the simulated data set

As stated previously [27], Friedman's method is fundamentally an infinitely sequential model in which the reaction sequence must by definition maintain the same order. Ordinarily, as for fossil fuels, the remaining reactivity in the reactivity distribution decreases with conversion, but for energetic material, the activation energy can decrease with conversion, thereby leading to the generation of highly acceleratory reaction characteristics under some circumstances. Using isoconversional kinetic parameters in an infinitely sequential mode works quite well in either case. One merely generates an effective first-order pre-exponential factor for each arbitrarily small fraction reacted interval and performs a sequence of first-order reaction calculations. A comparison of the isoconversional parameter calculations with the input model conversions is shown in Fig. 2.17. The agreement is excellent.

The lesson is that there are a variety of well-explored approaches to treat reactivity distributions, and some work better than others. Single, continuous activation energy distributions such as Gaussian, *n*th-order Gaussian, and Weibull

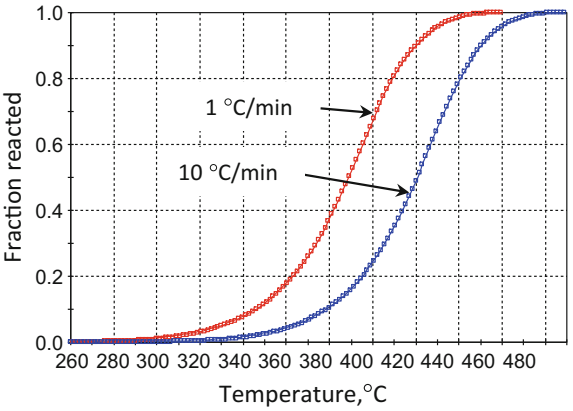

Fig. 2.17 Comparison of fractions reacted from the simulated data set with those calculated (*lines*) from Friedman isoconversional parameters derived from the simulated data set (*points*)

are not sufficiently flexible to achieve an excellent fit to real data from complex systems. In those cases, either the discrete model, the extended discrete model, or Friedman's isoconversional model are far superior, although multiple continuous distributions sometimes do well. The extended discrete and isoconversional methods may be advantageous in some circumstances (e.g., energetic materials) where it is important to account for the variability of the pre-exponential factor with activation energy, but the difference is ordinarily negligible within the range of calibration and small even when extrapolated to substantially different time-temperature regimes. The one situation where continuous distribution models are superior is for sparse data sets where there is insufficient information to calibrate either the discrete or isoconversional models. Regardless of which models are used, one must be careful not to over-interpret the model parameters.

2.7 Identifying and Fitting the Right Kinetic Model

People involved in kinetics can be categorized as users or musers [50]. Users use chemical kinetics for process design, petroleum exploration, or lifetime and safety evaluations. They need reliable algorithms. Theoretical rigor is important only to the extent it improves reliability. Musers muse over experimental and theoretical concepts. Many often consider only qualitative issues. Some musers come up with conceptual and algorithmic advances that are useful to users.

This section is directed towards users, not musers. Many of the initial steps of deriving a reliable model involve the same conceptual evaluation used by musers. However, once the correct conceptual model is chosen, users proceed to calibrate the conceptual model parameters so it can be useful. This often requires more sophisticated software than musers are willing to acquire. Even so, just because a person has powerful software does not mean they know how to use it effectively to derive practical and reliable models. Learning how to be effective is the objective here.

Guidance on how to collect meaningful data is given by Vyazovkin et al. [109] and only a few points are covered here. First and foremost, equipment must be properly calibrated to achieve accurate temperatures, and sample sizes must be small enough that thermal gradients during thermal transients do not invalidate the temperature measurement [110]. For ordinary materials, the product of sample size and heating rate should not exceed 100 mg °C/min [111]. For particularly endothermic or exothermic materials (e.g., explosives), that product should be 20–100 times lower, depending on the reaction enthalpy.

The next step in calibrating a model is to acquire the relevant data. That means gathering rate or conversion data over a wide range of temperatures and time (actually logarithmic time) to adequate decouple the pre-exponential and exponential dependences in the Arrhenius equation. The width of the required temperature or heating rate range depends on the reproducibility of a single determination [50, 111]. As is obvious from the isoconversional principle, one needs longer time

data at lower temperatures to achieve conversion levels that are helpful for decoupling conversion and temperature dependences.

For thermal analysis experiments, a properly conceived experimental plan will have experiments at multiple temperatures, multiple heating rates, or both. This provides a robust data set. Nonlinear temperature profiles, such as changing the temperature during the run to maintain an approximately constant reaction rate or a slow sinusoidal oscillation of the temperature superimposed upon a constant ramp, can also provide a good test of reaction models. In fact, the oscillating ramp (e.g., ~20 oscillations of 5–10 °C amplitude per ramp) samples both the activation energy and frequency factor at various extents of conversion, so a single experiment can derive kinetic parameters under ideal conditions.

Batch experiments are more problematic, in that often conversion is known only at the end of the experiment. Consequently, it is highly desirable to conduct multiple times at a given temperature, including longer times at lower temperatures. Sometimes batch experiments are conducted only at fixed time for various temperatures (e.g., 72 h for hydrous pyrolysis). Such data are useful for checking a model based on other information but are inadequate by themselves to calibrate a model because they cannot decouple temperature and conversion dependences.

The general concept for identifying and calibrating applied chemical kinetic models for condensed phase pyrolysis is shown in Fig. 2.18. First, one uses a variety of simple inspection methods to narrow the range of model possibilities. The first and most obvious step is to look at the data. This means plotting it in various ways, most likely as reaction rate or fraction converted as a function of time (or temperature in the case of a constant heating rate). Distinct humps or separate peaks at a constant heating rate indicate multiple processes, which should be modeled separately. Isothermal experiments are particularly helpful for identifying

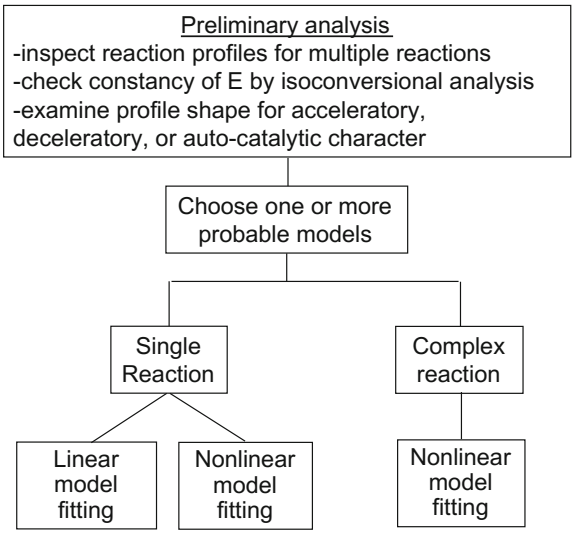

Fig. 2.18 General methodology for deriving reliable applied chemical kinetic models

acceleratory or sigmoidal characteristics that are harder to detect in rising temperature experiments. Recall that the acceleratory characteristics may not be evident on a linear time scale, and conversion versus logarithmic time is also important to examine. It is also important to know the exact thermal history for nominally isothermal experiments in order to separate acceleration during heat-up from true autocatalytic or related acceleration.

For the preliminary analysis, three methods are now explored in more depth. They are isoconversional methods, LLNL approximate (extended Kissinger) analyses, and reduced scale plots. The first two are useful only for thermal-analysis-type data, i.e., many data points.

Isoconversional methods were described in some detail earlier, but specific features are relevant at this stage of analysis. First, it is highly desirable to use both the Friedman method and one of the advanced integral methods. The ICTAC kinetics report [6] recommends either the Kissinger-Akahira-Sunose (KAS) method or one of Vyazovkin's methods. Kinetics2015 uses an iterative multi-heating rate version of the Coats-Redfern equation [4], which is slightly more accurate than the KAS method. Although it is discouraged to use many isoconversional methods (including the obsolete OFW method) and compare them in detail, it is useful to use both differential and integral methods, as they have different weaknesses and tend to fail under different circumstances.

The first question to address with isoconversional methods is whether A and E are roughly constant versus conversion or vary significantly. One must take into consideration problems with noise in the data that tend to make the values for the first and last 10 % unreliable, but they should not be discounted completely. If there is a change, is it gradual or can the timing of it be related to some feature in the data?

The LLNL approximate analyses were developed between 1986 and 1998 and are based on an extended Kissinger analysis of constant heating rate data.

1. The first step is to determine an initial estimate of the characteristic A and E for the reaction system using one of the Kissinger methods to derive first-order parameters for something around mid-conversion. Equation (2.24) is used for rate data, and Eq. (2.19) is used for cumulative reacted.
2. The next step is to calculate the first-order rate curve from these parameters and compare it to the measured curves. Two characteristics are monitored: profile width and profile asymmetry. If the profile is narrower than a first-order reaction ($\rho < 1$), it is either autocatalytic or nth-order with n less than one. If it is wider ($\rho > 1$), it is some type of distributed reactivity reaction.
3. Profile asymmetry relative to a first-order reaction is then used in combination with relative width to estimate parameter values for various models, including the extended Prout-Tomkins model, nth-order, and Gaussian and Weibull distribution models.

Figure 2.19 shows the fields of relevance for the various models, and Table 2.3 shows the algorithms used for the model parameter estimates for the Gaussian

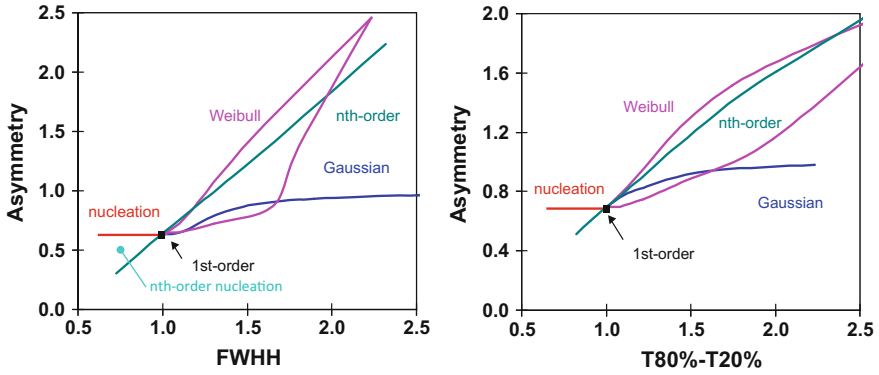

Fig. 2.19 Plots of asymmetry versus relative reaction profile width to help determine the relevant model needed for further refinement. For rate data, the asymmetry is $(T_{high} - T_{max})/(T_{max} - T_{low})$, where T_{high} and T_{low} are the temperatures at 25 % of the maximum rate. For fraction reacted data, asymmetry is $(T_{0.9} - T_{0.5})/(T_{0.5} - T_{0.1})$. In both cases, the relative profile width is the experimental value divided by the calculated width of a first-order reaction having the same A and E values. Reproduced courtesy of LLNL

Table 2.3 Examples of equations used to estimate selected model parameters in Kinetics2015, plus the simpler original algorithm used to estimate σ

Parameter	Rate data
First-order A and E	$\ln(\beta/T_{max}^2 = -E/RT_{max} + \ln(AR/E)$
Gaussian σ (orig)	$\sigma = -1.1/\rho^3 - 0.66/\rho^{30} + 2.88\rho - 1.12$
Gaussian σ	$\sigma = \{6.41 \times 10^6[(\rho - 1)\beta^{3000/\rho E}/E^{1.2} - 3.7 \times 10^9]\}^{0.54} + 7.14 \times 10^9 [(\rho - 1)^2\beta^{12000/\rho E}/E^{2.2}$
Gaussian A	$A_\sigma = A\{1 - 0.4[1 - \exp(\sigma/2.5)]\}$
Reaction order n	$n = (asym/0.64)^{0.78}$
Growth order m	$m = 1 - \rho^{1.92}/n$
ePT A	$A_{ePT} = A/(1 - m + 0.17m^2)$

distribution and ePT models. Comparable correlations are used for the Weibull model and for all models using fraction reacted data.

Reduced scale plots originated as a way to collapse conversion data for different temperatures onto a common plot on which their shapes can be compared to each other and to common reaction models [61]. Commonly, times for 50 or 90 % conversion are used for the scaling parameter. Recently, there has been more emphasis on plotting certain rate and conversion functions versus conversion. Several examples are given by Vyazovkin [6].

A simple starting point is to consider plotting the reaction rate for constant heating as a function of conversion. Such a plot is shown in Fig. 2.20 for three

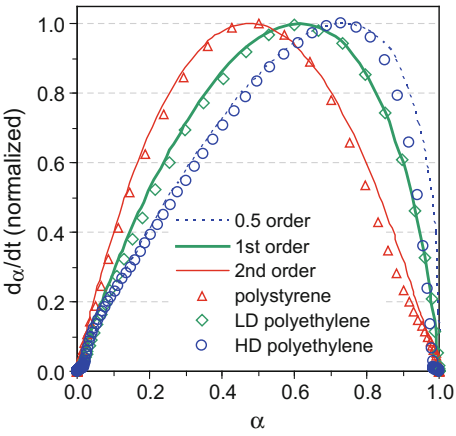

Fig. 2.20 Plot of normalized reaction rate versus conversion, which removes profile width effects to reflect one aspect of the appropriate reaction model. Reproduced courtesy of LLNL

polymers with different reaction shapes [6]. Such a plot is an alternative to the approach in Fig. 2.19 for evaluating the profile shape against selected model shapes, shown here for *n*th-order reactions. The decrease of nucleation-growth character is not captured in such a plot, as it affects profile width but not profile shape for a constant heating rate.

A different approach is to normalize the reaction rate or fraction reacted to unity at 50 % conversion. This works well when one has a good way to determine complete conversion, which is not always the case for mixtures reacted at constant temperature or where the amount of residue depends on the heating conditions. Nevertheless, it is often a good approach for identifying plausible models. Such normalized master curves for various models are shown in Fig. 2.21.

A limitation of the approaches in Figs. 2.19 and 2.20 is that they work only for constant heating rates. Similarly, the approaches shown in Figs. 2.2, 2.7 and 2.8 work only for isothermal conditions. The curves in Fig. 2.21 can be used directly only for isothermal data, but a method has been developed for their use for arbitrary thermal histories [112]. For the rate master curve, the method is conceptually simple. One first does an isoconversional or Kissinger kinetic analysis to generate an activation energy near mid conversion and then uses it to calculate what the reaction rate would have been had the temperature been the same as at mid-conversion. This gives the relation

$$Generalized\ Reduced\ Reaction\ Rate = \frac{(d\alpha/dt)_i}{(d\alpha/dt)_{0.5}} exp\left[\frac{E}{R}\left(\frac{1}{T_i} - \frac{1}{T_{0.5}}\right)\right] \qquad (2.49)$$

where the subscript i indicates the rate and temperature at the ith data point and the subscript 0.5 indicates the rate and temperature at 50 % conversion. Details on the integral method are given by Gotor et al. [112] and an example is given by Sánchez-Jiménez et al. [97] for cellulose heated at a constant heating rate showing its similarity to nucleation-growth and random scission models.

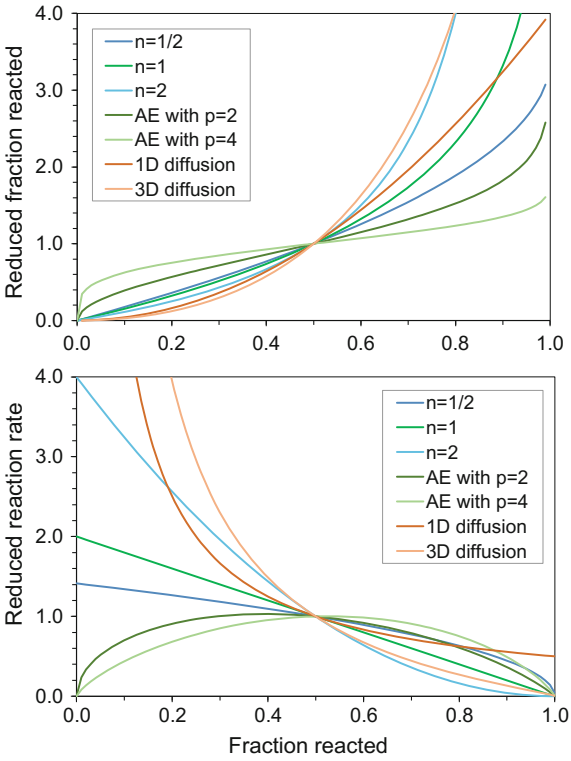

Fig. 2.21 Master plots of reaction rates and fractions reacted for various reaction models

A comparable plot is shown in Fig. 2.22 for the sample Kel-F data shown in Fig. 2.10. (In this case, the activation energy is essentially constant, so the calculation of the reduced reaction rate is simple.) The constant heating rate and isothermal data collapse on the same general curve. For the models shown in Fig. 2.21, the match is best with the Avrami-Erofe'ev model with $p = 2$, but the peak is clearly skewed to lower conversion. Comparing these plots to the cellulose data of Sánchez-Jiménez et al. [97] the agreement is actually better for a random scission kinetic model or an ePT model, although the two are similar in many respects.

Many synthetic polymers are likely to follow a nucleation-growth model. Figure 2.23 shows the variety of profile shapes available via the ePT model, all of which have an acceleratory phase. The initial rate is determined by the quantity $1 - q$, which is proportional to the ratio of initiation to propagation rates. Plotting the experimental data on this type of plot can help identify an appropriate model and initial guesses for non-linear regression. However, it is equally important to consider the profile width as well as shape. That is particularly easy using a plot like that in Fig. 2.19.

Sanchez-Jimenez et al. [113] recently used a simple random scission model adapted from the work of Simha and Wall [114] to fit polymer decomposition data.

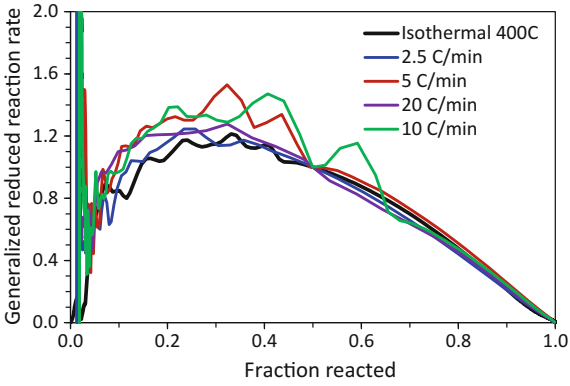

Fig. 2.22 Generalized reaction rate master plot for Kel-F 800

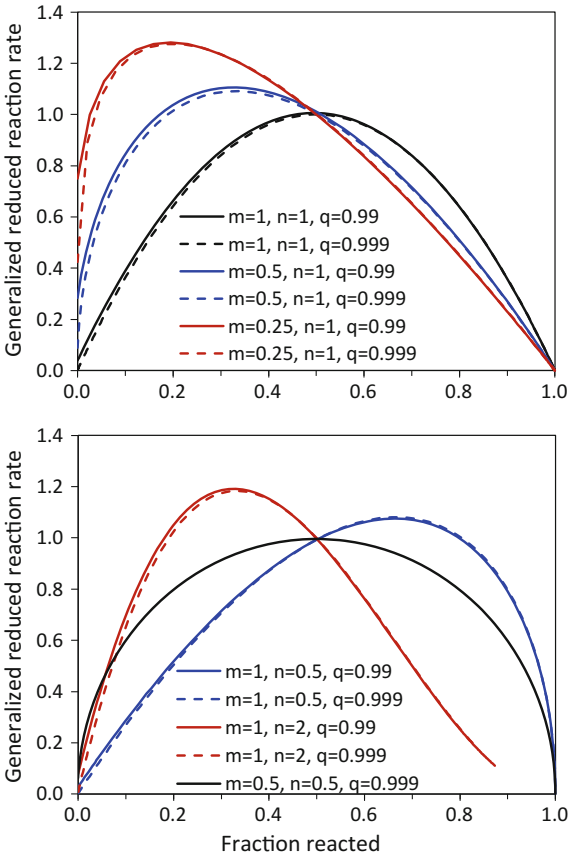

Fig. 2.23 Various profile shapes available via the ePT nucleation-growth model. Note that these curves do not address profile width, which is equally important

Although Burnham et al. [79] had already made the qualitative connection, Sanchez-Jimenez et al. provide a more quantitative comparison. For the chain-length parameter L favored in that paper, the random scission model reduces to $f(\alpha) = 2(\alpha^{1/2} - \alpha)$. They report $n = 1.12$ and $m = 0.40$ as the equivalent ePT parameters from their linear regression method. Similarly, Kinetics2015 obtains $n = 1.13$ and $m = 0.48$. A point rarely mentioned in the literature is that sigmoidal reactions need to start with a finite amount of reaction or the rate will be identically zero for all time. In this case, $\alpha = 0.001$ was assumed at time zero to create the simulated data, which corresponds to $q = 0.999$ in the non-linear regression.

The application of generalized reduced reaction rate plots is also instructive for materials with a reactivity distribution. Since, by definition, it is likely that the activation energy will increase with conversion, it is not immediately obvious whether one should use the mean activation energy or the isoconversional activation energy at the indicated level of conversion. However, numerical studies show unambiguously that the mean activation energy is to be used throughout. A reactivity distribution model is clearly more deceleratory than a first-order reaction under isothermal conditions, but using the activation energy at the *i*th-level of conversion gives an acceleratory phase, while using the mean energy gives superimposable reaction rate plots for isothermal and constant-heating-rate conditions.

A comparison of this method for model Gaussian reactions, a high-volatile coal, and a petroleum source rock are shown in Fig. 2.24. The Gaussian model used a mean activation energy of 30,070 K, a frequency factor of 2×10^{16} s^{-1}, and an energy distribution of 4.8 % of the mean. The petroleum source rock is fitted well by a Gaussian energy distribution model having an energy distribution of 1.7 % of the mean. The Pittsburgh #8 high volatile bituminous coal is more problematic, in that its shape is not well represented by a Gaussian distribution, so depending on the fitting method, one gets distributions of 3.5–7 % of the mean energy. That is qualitatively consistent with its similarity to the 4.8 % Gaussian generalized reaction rate plot.

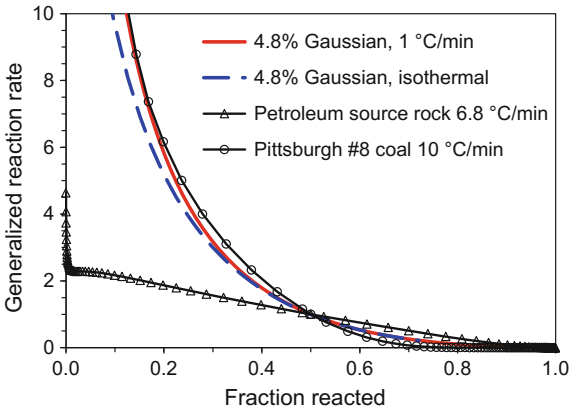

Fig. 2.24 Generalized reaction rate master plot for a Gaussian energy distribution model and data for a coal and petroleum source rock

Once a model has been selected, one can proceed to nonlinear regression to optimize the model parameters. Good initial parameter estimates for refinement must be generated by some combination of the methods outlined above, as poor estimates may lead to a false minimum or complete failure of convergence. Our experience is that no more than 4–5 parameters should be refined at once, so holding some constant and working manually toward a global minimum is warranted for complex models, particularly those involving overlapping reaction profiles. Although it might be nice to have an explicit recipe, each situation is slightly different, and one must learn from experience and comparison to the approaches of others.

Another consideration is what objective function to minimize. Ordinarily, one would fit rate data to a rate equation by minimizing those residuals and fit fraction reacted data to an integrated equation by minimizing those residuals.[1] It is important always to collect the complete thermal history and integrate the rate laws over that thermal history rather than assume an isothermal or constant heating rate analytical expression. Such approximations are not needed with today's computational power and can lead to substantial errors in kinetic parameters, particularly for nominally isothermal experiments.

However, data can be integrated or differentiated to obtain the other form to regress, and there may be reasons to do so. If so, one should be sure to use mathematical algorithms for differentiating and integrating that do not introduce numerical errors. It may also be valuable to minimize the residuals simultaneously on both rates and integrals, because they are sensitive to different aspects of the reaction data. A final caution is that it is ordinarily best to weight each experiment equally rather than each data point equally, because slower experiments typically have more data points but do not contain significantly more information to drive the optimization.

Exercises

1. What can and cannot be learned about global chemical kinetic parameters from transition-state theory?
2. Explain one example for which the approximation $d\alpha/dt = k(T)f(\alpha)$ is not valid.
3. Show that the formulas for a pseudo *n*th-order reaction in Table 2.1 are equivalent to Eq. (2.11) in Burnham and Braun, *Energy & Fuels* **13**, 1–22 (1999).
4. Kinetic T_{max} values of a first-order reaction are 434.5, 460.6, and 488.6 °C at constant heating rates of 2, 8 and 32 °C/min. Write a simple spreadsheet or other program for Kissinger's method and calculate *A* and *E*.
5. If there is a measurement error for T_{max} of +1 °C at 32 °C/min and −1 °C at 2 °C/min, what are the resulting *A* and *E*? Now repeat the calculation with the

[1]The presumption here in both cases is that the fit will be to the data as collected and not a logarithmic form or a linearized transformation. Such manipulation tends to magnify the importance of data with large error bars, leading to poorer agreement on the most important portions.

signs of the temperature errors reversed. Plot the ln(A) versus E for these two pairs along with the pair from problem 4. What does it mean?

6. Write a spreadsheet or other program to calculate the reaction rate and fraction reacted of a first-order reaction for (at least) a constant heating rate. Justify your choice of integration method. Generate simulated data for three parallel reactions with $A = 1{\times}10^{13}$ s^{-1}, E = 49, 51, and 53 kcal/mol, and weighting factors of 0.2, 0.5 and 0.3, respectively, at 1, 5 and 25 °C/min. What are the temperatures for 50 % conversion at the three heating rates?
7. For the simulated data from problem 5, what is the full width at half height of the reaction rate profile at 5 °C/min? What is the full width at half height of the reaction rate profile for the principal reaction channel (51 kcal/mol) at the same heating rate? From the ratio of the two profile widths and the simpler equation in Table 2.3, what is an estimate for the Gaussian E-distribution parameter, σ.
8. For the simulated data from problem 5, use Friedman's method to calculate the instantaneous first-order A and E values at 10, 30, 50, 70 and 90 % conversion.
9. What is the purpose of the parameter q in the extended Prout-Tompkins model (Eq. 2.38) and what is the approximation associated with it having a constant value.
10. Write a spreadsheet or other program to calculate the reaction rate and fraction reacted for the extended Prout-Tompkins model (Eq. 2.38) for an arbitrary thermal history. Plot the reaction rate curves at 480 °C and 10 °C/min for $A = 1{\times}10^{14}$ s^{-1}, E = 54, q = 0.99, and m = 0.0, 0.5, and 1.0. Plot the isothermal times between 10 and 50 % conversion versus the profile full widths at half height for m = 0.0, 0.5 and 1.0. Why does the curve have a negative slope?

References

1. Originally Published by S. Arrhenius in Z. Phys. Chem. **4**, p. 226, It is covered in any undergraduate physical chemistry text (1889)
2. Boltzmann Distribution (2016), https://en.wikipedia.org/wiki/Boltzmann_distribution. Accessed 7 Aug 2016
3. Maxwell-Boltzmann Distribution (2016), https://en.wikipedia.org/wiki/Maxwell-Boltzmann_distribution. Accessed 7 Aug 2016
4. A.K. Burnham, R.L. Braun, Global kinetic analysis of complex materials. Energy Fuels **13**, 1–22 (1999)
5. Transition-state theory was first published by, H. Eyring in 1935, and its history is covered in a special journal issue in his memory by K.J. Laidler, M.C. King, The development of transition-state theory. J. Phys. Chem. **87**, 2657–2664 (1983)
6. S. Vyazovkin, A.K. Burnham, J.M. Criado, L.A. Perez-Maqueda, C. Popescu, N. Sbirrazzuoli, ICTAC recommendations for performing kinetic computations on thermal analysis data. Thermochim. Acta **520**, 1–19 (2011)
7. J.R. Frade, M. Cable, Theoretical solutions for mixed control of solid state reactions. J. Mat. Sci. **32**, 2727–2733 (1997)

8. Z. Du, A.F. Sarofim, J.P. Longwell, C.A. Mims, Kinetic measurement and modeling of carbon oxidation. Energy Fuels **5**, 214–221 (1991)
9. K.J. Jackson, A.K. Burnham, R.L. Braun, K.G. Knauss, Temperature and pressure dependence of *n*-hexadecane cracking. Org. Geochem. **23**, 941–953 (1995)
10. A.K. Burnham, R.K. Weese, A.P. Wemhoff, J.L. Maienschein, A historical and current perspective on predicting thermal cookoff behavior. J. Therm. Anal. Cal. **89**, 407–415 (2007)
11. E.A. Glascoe, J.M. Zaug, A.K. Burnham, Pressure-dependent decomposition kinetics of the energetic material HMX up to 3.6 GPa. J. Phys. Chem. A **113**, 13548–13555 (2009)
12. H. Freund, J.A. Couse, G.A. Otten, Effects of pressure on the kinetics of kerogen pyrolysis. Energy Fuels **7**, 1088–1094 (1993)
13. D.B. Anthony, J.B. Howard, Coal devolatilization and hydrogasification. AIChE J. **22**, 625–656 (1976)
14. E.A. Dorko, W. Bryant, T.L. Regulinski, Solid-state reaction kinetics. IV. Analysis of chemical reactions by means of the Weibull function. Anal. Calorim. **3**, 505–509 (1974)
15. R. Aris, Reactions in continuous mixtures. AIChE J. **35**, 539–548 (1989)
16. J.H. Flynn, The temperature integral—its use and abuse. Thermochim. Acta **300**, 83–92 (1997)
17. K.H. Van Heek, H. Juntgen, W. Peters, Kinetics of nonisothermal reactions, using thermal decomposition reactions as an example. Ber. Bunsenges. Physik. Chem. **71**, 113–121 (1967)
18. J.H. Campbell, G.J. Koskinas, N.D. Stout, Kinetics of oil generation from Colorado oil shale. Fuel **57**, 372–376 (1978)
19. A.W. Coats, J.P. Redfern, Kinetic parameters from thermogravimetric data. Nature **201**, 68–69 (1964)
20. C. Popescu, E. Segal, On the temperature integral in non-isothermal kinetics with linear heating rate. Thermochim. Acta **75**, 253–257 (1984)
21. G.I. Senum, R.T. Yang, Rational approximations of the integral of the Arrhenius function. J. Therm. Anal. **11**, 446 (1977)
22. L.A. Perez-Maqueda, J.M. Criado, The accuracy of Senum and Yang's approximations to the Arrhenius integral. J. Thermal Analysis **60**, 909–915 (2000)
23. R.L. Braun, A.K. Burnham, Analysis of chemical reaction kinetics using a distribution of activation energies and simpler models. Energy Fuels **1**, 153–161 (1987)
24. W. Gautschi, W.F. Cahill, in *Handbook of Mathematical Functions*; ed. by M. Abramowitz, I.A. Stegun. (National Bureau of Standards, AMS 55, Washington, D. C, 1964), pp. 228–231
25. A.C. Hindmarsh, LSODE and LSODI two new. Initial value ordinary Differential Equation Solvers. ACM SIGNUM Newsl. **15**(4), 10–11 (1980)
26. S.V. Gulikeri, D. Luss, Analysis of activation energy of grouped parallel reactions. AIChE J. **18**, 277–282 (1972)
27. A.K. Burnham, L.N. Dinh, A comparison of isoconversional and model-fitting approaches to kinetic parameter estimation and application predictions. J. Therm. Anal. Cal. **89**, 479–490 (2007)
28. S. Vyazovkin, *Isoconversional Kinetics of Thermally Stimulated Processes* (Springer, 2015)
29. H.L. Friedman, Kinetics of thermal degradation of char-forming plastics from thermogravimetry: application to a Phenolic Plastic. J. Polym. Sci., Part C. **6**, 183–195 (1964)
30. T. Ozawa, A new method for analyzing thermogravimetric data. Bull. Chem. Soc. Jpn. **38**, 1881 (1965)
31. J.H. Flynn, L.A. Wall, A quick, direct method for the determination of activation energy from thermogravimetric data. Polymer Lett. **4**, 323–328 (1966)
32. J.H. Flynn, The isoconversional method for determination of energy of activation at constant heating rates: corrections for the Doyle approximation. J. Therm. Anal. **27**, 95–102 (1983)
33. J.H. Flynn, Early papers by Takeo Ozawa and their continuing relevance. Thermochim. Acta **282**(283), 35–42 (1996)
34. C.D. Doyle, Estimating isothermal life from thermogravimetric data. J. Appl. Polym. Sci. **6**, 639–642 (1962)

35. T. Ozawa, Estimation of activation energy by isoconversional methods. Thermochim. Acta **203**, 159–165 (1992)
36. M.J. Starink, Activation energy determination for linear heating experiments: a comparison of the accuracy of isoconversional methods. Thermochim. Acta **404**, 163–176 (2003)
37. S. Vyazovkin, Modification of the integral isoconversional procedure to account for variation in the activation energy. J. Comput. Chem. **22**, 178–183 (2001)
38. M.E. Brown, M. Maciejewski, S. Vyazovkin, R. Nomen, J. Sempere, A. Burnham, J. Opfermann, R. Strey, H.L. Anderson, A. Kemmler, R. Drueleers, J. Janssens, H.O. Desseyn, C.-R. Li, T.B. Tang, B. Roduit, J. Malek, T. Mitsuhashi, Computational aspects of kinetic analysis. Part A: the ICTAC Kinetics Project—data, methods and results. Thermochim. Acta **355**, 125–143 (2000)
39. K. Miura, A new and simple method to estimate f(E) and k0(E) in the distributed activation energy model from three sets of experimental data. Energy Fuels **9**, 302–307 (1995)
40. K. Miura, T. Maki, A simple method for estimating f(E) and k0(E) in the distributed activation energy model. Energy Fuels **12**, 864–869 (1998)
41. V. Vand, A theory of the irreversible electric resistance changes of metallic films evaporated in vacuum, Proc. Phys. Soc. (London, 1943), pp. 222–246
42. http://www.geoisochem.com/software/kinetics2015/index.html. Accessed 7 Aug 2016
43. http://www.akts.com/akts-thermokinetics-tga-dsc-dta-tma-ftir-ms/download-tga-dsc-dta-tma-ms-ftir-akts-thermokinetics-software.html. Accessed 7 Aug 2016
44. H.E. Kissinger, Reaction kinetics in differential thermal analysis. Anal. Chem. **29**, 1702–1706 (1957)
45. H.E. Kissinger, Variation of peak temperature with heating rate in differential thermal analysis. J. Res. Nat. Bur. Stand. **57**, 217–221 (1956)
46. D. Chen, X. Gao, D. Dollimore, A generalized form of the Kissinger equation. Thermochim. Acta **215**, 109–117 (1993)
47. P.A. Redhead, Thermal desorption of gases. Vacuum **12**, 203–211 (1962)
48. V. Dieckmann, Modelling petroleum formation from heterogeneous source rocks: the influence of frequency factors on activation energy distribution and geological prediction. Mar. Petrol. Geol. **22**, 375–390 (2005)
49. Simple Linear Regression, http://en.wikipedia.org/wiki/Simple_linear_regression. Accessed 6 Mar 2014
50. A.K. Burnham, Obtaining reliable phenomenological chemical kinetic models for real-world applications. Thermochim. Acta **597**, 35–40 (2014)
51. A. Yelon, E. Sacher, W. Linert, Comment on the mathematical origins of the kinetic compensation effect parts 1 and 2 by P.J. Barrie, Phys. Chem. Chem. Phys. **14**, 318 and 327 (2012). Phys. Chem. Chem. Phys. **14**, 8232–8234 (2012)
52. P.J. Barrie, Reply to comment on the mathematical origins of the kinetic compensation effect. parts 1 and 2 by A. Yelon, E. Sacher, W. Linert, Phys. Chem. Chem. Phys. **14**, (2012). Phys. Chem. Chem. Phys. **14**, 8235–8236 (2012)
53. Non-linear Least Squares, http://en.wikipedia.org/wiki/Non-linear_least_squares. Accessed 7 Aug 2016
54. Levenberg-Marquardt Algorithm, http://en.wikipedia.org/wiki/Levenberg%E2%80%93Marquardt_algorithm. Accessed 7 Aug 2016
55. C.C. Lakshmanan, M.L. Bennett, N. White, Implications of multiplicity in kinetic parameters to petroleum exploration: distributed activation energy models. Energy Fuels **5**, 110–117 (1991)
56. J. Hillier, T. Bezzant, T.H. Fletcher, Improved method for the determination of kinetic parameters from non-isothermal thermogravimetric analysis (TGA) data. Energy Fuels **24**, 2841–2847 (2010)
57. https://www.netzsch-thermal-analysis.com/us/products-solutions/software/netzsch-advanced-software/thermokinetics/. Accessed 7 Aug 2016
58. D.A. Ratkowsky, *Handbook of Nonlinear Regression Models* (Marcel Dekker, 1990), pp. 36–48

59. A.K. Burnham, An *n*th-order Gaussian energy distribution model for sintering. Chem. Eng. J. **108**, 47–50 (2005)
60. B. Roduit, M. Hartmann, P. Folly, A. Sarbach, R. Baltensperger, Prediction of thermal stability of materials by modified kinetic and model selection approaches based on limited amount of experimental points. Thermochim. Acta **579**, 31–39 (2014)
61. W.E. Brown, D. Dollimore, A.K. Galway, in *Comprehensive Chemical Kinetics*, ed. by C.H. Bamfor, C.F. Tipper. Reactions in the solid state, vol. 22 (Elsevier, 1980), pp 49–65
62. M. Avrami, Kinetics of phase change, I. General theory, J. Chem. Phys. **7**, pp. 1103–1112 (1939); II. Transformation-time relation for random distribution of nuclei, J. Chem. Phys. **8**, pp. 212–224 (1940); III. Granulation, phase change, and microstructure, J. Chem. Phys. **8**, pp. 177–184
63. W. Johnson, R. Mehl, Reaction kinetics in processes of nucleation and growth. Trans. AIME **135**, 416–442 (1939)
64. A. Kolmogorov, A statistical theory for the recrystallization of metals, Akad. Nauk. SSSR, Izv. Ser. Matem. **1**, pp. 355–359 (1937)
65. B.V. Erofe'ev, A generalized equation of chemical kinetics and its application in reactions involving solids, C.R. Dokl. Akad. Sci. USSR **52**, pp. 511–514 (1946)
66. E.G. Prout, F.C. Tompkins, The thermal decomposition of potassium permanganate. Trans. Faraday Soc. **40**, 488–498 (1944)
67. U. Retter, D. Vollhardt, Chain nucleation: a critical consideration of Prout and Tompkins' Law. Langmuir **8**, 1693–1694 (1992)
68. J. Šesták, G. Berggren, Study of the kinetics of the mechanism of solid-state reactions at increasing temperatures. Thermochim. Acta **3**, 1–12 (1971)
69. J.B. Austin, R.L. Rickett, Kinetics of the decomposition of austenite at constant temperature, AIME Technical publication. **964,** p. 20 (1938). Trans. AIME **135,** pp. 396–415
70. E.G. Prout, F.C. Tompkins, The thermal decomposition of silver permanganate. Trans. Far. Soc. **42**, 468–472 (1946)
71. B.V. Erofe'ev, in *Reactivity of Solids, Proceedings of the 4th Intl. Symp.,* (Elsevier, Amsterdam, 1961) pp. 273–282
72. M.A. Arshad, A. Maaroufi, Relationship between Johnson-Mehl-Avrami and Šesták-Berggren models in the kinetics of crystallization in amorphous materials. J. Non-Crystalline Solids **413**, 53–58 (2015)
73. N.S. Akulov, *Basics of Chemical Dynamics* (in Russian) (Moscow State University, 1940)
74. M. Rios-Fachal, C. Garcia-Fernandez, J. Lopez-Beceiro, S. Gomez-Barreiro, J. Tarrio-Saavedra, A. Ponton, R. Ariaga, Effect of nanotubes on the thermal stability of polystyrene, J. Therm. Anal. Cal. **113**, 481–487 (2013)
75. J. Tarrio-Saavedra, J. Lopez-Beceiro, S. Naya, M. Francisco-Fernandez, R. Artiaga, Simulation study for generalized logistic function in thermal data modeling. J. Therm. Anal. Cal. **118**, 1253–1268 (2014)
76. A.K. Burnham, Use and misuse of logistic equations for modeling chemical reactions, J. Therm. Anal. Cal. (2015)
77. Cheminform, St. Petersburg (CISP) Ltd, 197198, (14, Dobrolubov Ave, Saint Petersburg, Russia)
78. M.E. Brown, The Prout-tompkins rate equation in solid-state kinetics. Thermochim. Acta **300**, 93–106 (1997)
79. A.K. Burnham, R.L. Braun, T.T. Coburn, E.I. Sandvik, D.J. Curry, B.J. Schmidt, R.A. Noble, An appropriate kinetic model for well-preserved algal kerogens. Energy Fuels **10**, 49–59 (1996)
80. F.O. Rice, K.F. Herzfeld, The thermal decomposition of organic compounds from the standpoint of free radicals. VI. The mechanism of some chain reactions, J. Amer. Chem. Soc. **56**, 284–289 (1934)
81. J.H. Flynn, R.E. Florin, in *Pyrolysis and GC in polymer analysis*, ed. by S.A. Liebman, E. J. Levy. Degradation and pyrolysis mechanisms, (Marcel Dekker, 1985) pp. 149–208

82. R.E. Lyon, M.T. Takemori, N. Safronava, S.I. Stoliarov, R.N. Walters, A molecular basis for polymer flammability. Polymer **50**, 2608–2617 (2009)
83. L.A. Wall, in *Analytical Chemistry of Polymers, Part II*, Chapter 5, ed. by G.M. Kline. Pyrolysis,(Academic Press, 1962) pp. 181–248
84. L.A. Wall, S. Straus, Pyrolysis of polyolefins. J. Polym. Sci. **44**, 313–323 (1960)
85. A.K. Burnham, R.L. Braun, *Kinetics of Polymer Decomposition* (Lawrence Livermore National Laboratory Rept. UCID-21293, 1987) p. 28
86. A.K. Burnham, R.L. Braun, R.W. Taylor, T.T. Coburn, Comparison of isothermal and nonisothermal pyrolysis data with various rate mechanisms: implications for kerogen structure. Prepr. ACS Div. Petrol. Chem. **34**(1), 36–42 (1989)
87. A.K. Burnham, Application of the Šesták-Berggren equation to organic and inorganic materials of practical interest. J. Therm. Anal. Cal. **60**, 895–908 (2000)
88. A.K. Burnham, R.K. Weese, Kinetics of thermal degradation of explosive binders Viton A, Estane, Kel-F. Thermochim. Acta **426**, 85–92 (2005)
89. J.D. Nam, J.C. Seferis, Generalized composite degradation kinetics for polymeric systems under isothermal and nonisothermal conditions. J. Poly Sci. B Poly. Phys. **30**, 455–463 (1992)
90. J.G. Reynolds, A.K. Burnham, Pyrolysis decomposition kinetics of cellulose-based materials by constant heating rate micropyrolysis. Energy Fuels **11**, 88–97 (1997)
91. R. Capart. L. Khezami, A.K. Burnham, Assessment of various kinetic models for the pyrolysis of a microgranular cellulose. Thermochim. Acta. **417**, 79–89 (2004)
92. D. Dollimore, B. Holt, Thermal degradation of cellulose in nitrogen. J. Poly. Sci. **11**, 1703–1711 (1973)
93. M. Grønli, M.J. Antal Jr., G. Várhegyi, A round-robin study of cellulose pyrolysis kinetics by thermogravimetry. Ind. Eng. Chem. Res. **38**, 2238–2244 (1999)
94. A.K. Burnham, X. Zhou, L.J. Broadbelt, Critical review of the global chemical kinetics of cellulose thermal decomposition. Energy Fuels **29**, 2906–2918 (2015)
95. S. Kim, Y. Eom, Estimation of kinetic triplet of cellulose pyrolysis reaction from isothermal kinetic results. Kor. J. Chem. Eng. **23**, 409–414 (2006)
96. H. Barud, C. Riberio, J. Capella, M.S. Crespi, S. Ribeiro, Y. Messadeq, Kinetic parameters for thermal decomposition of microcrystalline, vegetal, and bacterial cellulose. J. Therm. Anal. Cal. **105**, 421–426 (2011)
97. P. Sanchez-Jimenez, L. Perez-Maqueda, A. Perejon, J.M. Criado, Generalized master plots as a straightforward approach for determining the kinetic model: the case of cellulose pyrolysis. Thermochim. Acta **552**, 54–59 (2013)
98. F.H. Constable, The mechanism of catalytic decomposition. Proc. Royal. Soc. A **108**, 355–378 (1925)
99. G.J. Pitt, The kinetics of the evolution of volatile products from coal. Fuel **41**, 267–274 (1962)
100. P. Hanbaba, *Reaktionkinetische Untersuchungen sur Kohlenwasserstoffenbindung aus Steinkohlen bie niedregen Aufheizgeschwindigkeiten*. Dissertation, University of Aachen, (1967)
101. P. Ungerer, R. Pelet, Extrapolation of the kinetics of oil and gas generation from laboratory experiments to sedimentary basins. Nature **327**, 52–54 (1987)
102. L. Kolar-Anić and S. Veljković, Weibull distribution and kinetics of heterogeneous processes. J. Chem. Phys. **63**, pp. 663–668 (1975); Statistical foundations of heterogeneous kinetics, ibid., pp 669–673
103. T.C. Ho, R. Aris, On apparent second-order kinetics. AIChE J. **33**, 1050–1051 (1987)
104. J. Cai, R. Liu, Weibull mixture model for modeling nonisothermal kinetics of thermally stimulated solid-state reactions: application to simulated and real kinetic conversion data. J. Phys. Chem. B. **111**, 10681–10686 (2007)
105. E.M. Suuberg, Approximate solution technique for nonisothermal, gaussian distributed activation energy models. Combust. Flame **50**, 243–245 (1983)

106. A.K. Burnham, R.L. Braun, H.R. Gregg, A.M. Samoun, Comparison of methods for measuring kerogen pyrolysis rates and fitting kinetic parameters. Energy Fuels **1**, 452–458 (1987)
107. P. Sundararaman, P.H. Merz, R.G. Mann, Determination of kerogen activation energy distribution. Energy Fuels **6**, 793–803 (1992)
108. J. Cai, T. Li, R. Liu, A critical study of the Miura-Maki integral method for the estimation of the kinetic parameters of the distributed activation energy model. Bioresour. Technol **102**, 3894–3899 (2011)
109. S. Vyazovkin, K. Chrissafis, M.L. Di Lorenzo, N. Koga, M. Pijolet, B. Roduit, N. Sbirrazzuoli, J.J. Sunol, ICTAC Kinetics Committee recommendations for collecting experimental thermal analysis data for kinetic computations. Thermochim. Acta **590**, 1–23 (2014)
110. R.E. Lyon, N. Safronova, J. Senese, S. Stoliarov, Thermokinetic model of sample response in nonisothermal analysis. Thermochim. Acta **545**, 82–89 (2012)
111. K.E. Peters, A.K. Burnham, C.C. Walters, Petroleum generation kinetics: single versus multiple heating-ramp open-system pyrolysis. AAPG Bull. **99**, 591–616 (2015)
112. F.J. Gotor, J.M. Criado, J. Malak, N. Koga, Kinetic analysis of solid-state reactions: the universality of master plots for analyzing isothermal and nonisothermal experiments. J. Phys. Chem. A **104**, 10777–10782 (2000)
113. P.E. Sanchez-Jimenez, L.A. Perez-Maqueda, A. Perejon, J.M. Criado, A new model for the kinetic analysis of thermal degradation of polymers driven by random scission. Poly. Degrad. Stab. **95**, 733–739 (2010)
114. R. Simha, L.A. Wall, Kinetics of chain depolymerization. J. Phys. Chem. **56**, 707–715 (1952)

http://www.springer.com/978-3-319-49633-7

Global Chemical Kinetics of Fossil Fuels
How to Model Maturation and Pyrolysis
Burnham, A.K.
2017, XII, 315 p. 202 illus., 101 illus. in color. With online files/update., Hardcover
ISBN: 978-3-319-49633-7